PROCEEDINGS A

royalsocietypublishing.org/journal/rspa

Research

Cite this article: Meng Y, Romero-García V, Gabard G, Groby J-P, Bricault C, Goudé S, Sheng P. 2022 Fundamental constraints on broadband passive acoustic treatments in unidimensional scattering problems. *Proc. R. Soc. A* **478**: 20220287.
https://doi.org/10.1098/rspa.2022.0287

Received: 2 May 2022
Accepted: 18 August 2022

Subject Areas:
applied mathematics, acoustics

Keywords:
acoustic metamaterials, causality and passivity constraints, sum rules, Herglotz functions

Author for correspondence:
Yang Meng
e-mail: mengyang2116@gmail.com

Electronic supplementary material is available online at https://doi.org/10.6084/m9.figshare.c.6176259.

THE ROYAL SOCIETY PUBLISHING

Fundamental constraints on broadband passive acoustic treatments in unidimensional scattering problems

Yang Meng[1], Vicente Romero-García[1,2], Gwénaël Gabard[1], Jean-Philippe Groby[1], Charlie Bricault[3], Sébastien Goudé[3] and Ping Sheng[4]

[1]Laboratoire d'Acoustique de l'Université du Mans, UMR CNRS 6613, Institut d'Acoustique—Graduate School, CNRS, Le Mans Université, Le Mans, France
[2]Departamento de Matemática Aplicada, Instituto Universitario de Matemática Pura y Aplicada, Universitat Politècnica de València, Camino de Vera, s/n, València 46022, Spain
[3]Vibrations and Acoustics Laboratory, Valeo Thermal Systems, Paris, France
[4]Department of Physics, Hong Kong University of Science and Technology, Clear Water Bay, Kowloon, Hong Kong, People's Republic of China

YM, 0000-0001-5646-462X; VR-G, 0000-0002-3798-6454; GG, 0000-0002-1527-4261; J-PG, 0000-0002-9308-8261; CB, 0000-0003-0420-5604; PS, 0000-0001-9000-6366

In a passive lossy acoustical system, sum rules derived from passivity explicitly relate the broadband response to the spatial dimension of the system, which provide important design criteria as well. In this work, the theory of Herglotz function is applied systematically to derive sum rules for unidimensional scattering problems relying on passive acoustic treatments which are generally made of rigid, motionless and subwavelength structures saturated by air. The rigid-boundary reflection, soft-boundary reflection and transmission problems are analysed. The derived sum rules are applied for guiding the designs of passive absorbers and mufflers: the required minimum space is directly predicted from the target (i.e. the desired absorption or transmission-loss spectra) without any specific design. Besides, it is possible to break this type of sum rules and fundamental constraints in particular cases.

This property, if well used, could result in ultra-compact absorbers working at long wavelength up to infinity.

1. Introduction

Passivity is an inherent property satisfied by many physical systems which do not produce energy by themselves. In particular, for a continuous, causal, linear and time-translational invariant system, passivity may lead to sum rules and impose fundamental constraints on the system. Generally speaking, sum rules are integral identities of the form $\int_0^\infty \omega^{-n} A(\omega)\,\mathrm{d}\omega = C$, where ω refers to the angular frequency, $A(\omega)$ is the considered response function, n is an integer included in the weighting factor ω^{-n} and the constant C is determined by the static and dynamic properties of the system. Particularly, for the sum rules derived from passivity, $A(\omega) \geq 0$, since the definition of a passive system is closely related to non-negative valued functions [1–4]. Then, the constant $C \geq 0$. And moreover, the integration within a finite frequency range provides a lower bound of C, which indicates a fundamental constraint satisfied by the passive system.

In order to derive sum rules and fundamental constraints of a given system, the Kramers–Kronig relations [5,6], the Bode gain-phase relation (or modified Kramers–Kronig relation) [7–9] and the superconvergence theorem [3,10–12] are commonly adopted. Examples can be found in network theory [13,14], optics [15], electromagnetism [16], acoustics [17–19], nuclear physics [20], feedback control systems and filters [21], etc. Note however that additional assumptions are usually made on the considered systems [2,15]. For instance, the response function is assumed to be a rational function in order to apply the Cauchy integral formula [2]. To consider more general cases with non-rational response functions for instance, one can build on the mathematical framework developed by Bernland *et al.* [2]. This approach relies on the properties of Herglotz functions [15,22] and has been used for various applications in electromagnetism, considering both lossless and lossy systems [3,23–26].

In contrast to electromagnetism, viscothermal losses usually play significant roles in the designs of passive treatments when we focus on acoustical systems in air, e.g. broadband absorbers [27–31], silencers [32,33], meta-diffusers [34,35], etc. See [36–40] and the references therein for other applications. Moreover, in lossy acoustical systems, the static/dynamic limits of the system response (and the aforementioned integral constant C) can be explicitly expressed by relevant spatial dimensions (i.e. total length or volume) as well as lumped structural parameters (i.e. porosity, tortuosity, etc.) of the system. Note that although these lumped parameters are unknowns without a specific design, their ranges and bounds are well known, e.g. $(0, 1]$ and $[1, \infty)$ for the porosity and the tortuosity, respectively [41]. Thus, this feature of lossy acoustical systems allows *a priori* estimates on the required spatial dimensions for any given target spectrum, which is of primary importance for the design of subwavelength passive treatments: whenever some information of the relevant response function (i.e. the design target) is known or assumed within finite frequency bands, sum rules of the system can be directly used to evaluate the lower bound of the required treatment size.

For most of the commonly used acoustical treatments, the system response functions are not rational functions, such as the acoustic impedance of a quarter-wavelength resonator, which is a cotangent function of frequency, and the radiation impedance of a baffled circular piston or orifice, which is related to Bessel functions [42]. Thus, in this work, we revisit the generalized theory based on the Herglotz functions [2] to derive and analyse the sum rules and fundamental constraints for lossy acoustical systems in unidimensional scattering problems. In §2, the mathematical framework of the theory of Herglotz function is recalled from [2]. The transfer matrix modelling of the considered scattering problems is described in §3a. The sum rules and fundamental constraints are then derived and discussed for a rigid-boundary reflection problem (§3b), a soft-boundary reflection problem (§3c) and a transmission problem (§3d). In §4, two specific examples are given to explain how to evaluate the required minimum treatment size by using these sum rules. Conclusions are drawn in §5. Further validation and

parametric studies of the derived sum rules are also provided in the electronic supplementary material.

2. Sum rules and fundamental constraints for a passive unidimensional system

For a continuous, causal, linear and time-translational invariant system, the output of the system $Y(t)$ can be expressed as a convolution between the input $X(t)$ and Green's function $G(t)$:

$$Y(t) = \int_0^\infty G(\tau)X(t-\tau)\,\mathrm{d}\tau, \tag{2.1}$$

where τ is the retarded time. Due to the causality of the system, $G(\tau) = 0$ for $\tau < 0$. After a time-domain Fourier transform, the convolution reduces to a product in the frequency domain that provides the definition of the frequency response function

$$\tilde{G}(\omega) = \frac{\tilde{Y}(\omega)}{\tilde{X}(\omega)}. \tag{2.2}$$

Note that in this work, we use the following Fourier transformation pair:

$$\tilde{f}(\omega) = \int_{-\infty}^{+\infty} f(t)\,\mathrm{e}^{\mathrm{i}\omega t}\,\mathrm{d}t \quad \text{and} \quad f(t) = \frac{1}{2\pi}\int_{-\infty}^{+\infty} \tilde{f}(\omega)\,\mathrm{e}^{-\mathrm{i}\omega t}\,\mathrm{d}\omega. \tag{2.3}$$

With the response function well defined, two equivalent definitions of the passivity of a system are generally considered, namely the admittance/impedance passivity and the scattering passivity [1–4]. For unidimensional scattering problems, the passivity of the system ensures that the flux of acoustic energy into the surface remains non-negative. When the surface admittance $\eta(\omega)$, or the impedance $\zeta(\omega) = 1/\eta(\omega)$ is the relevant frequency response function, the sign of the resistive part of the response function is therefore fixed (either non-negative or non-positive) depending on the definitions of η and ζ. Based on the non-negative-resistive-part definition, the admittance/impedance passivity implies that

$$\mathrm{Re}[\eta(\omega)] \geq 0 \quad \text{and} \quad \mathrm{Re}[\zeta(\omega)] \geq 0. \tag{2.4}$$

When enforcing the scattering passivity of the system, the reflection and transmission coefficients, $R(\omega)$ and $T(\omega)$, should be such that $0 \leq |R(\omega)|^2 + |T(\omega)|^2 \leq 1$, i.e. $-\ln[|R(\omega)|^2 + |T(\omega)|^2] \geq 0$, or separately, $0 \leq |R(\omega)| \leq 1$, and $0 \leq |T(\omega)| \leq 1$, so that scattering passivity results in

$$-\ln|R(\omega)| \geq 0 \quad \text{and} \quad -\ln|T(\omega)| \geq 0. \tag{2.5}$$

These relations state that the energy output of the system cannot exceed the input energy.

Herglotz functions are particularly useful to analyse the response of a passive system, since they are directly related to non-negative valued functions. By definition, a Herglotz function $H(\omega)$ is a holomorphic function in the upper half complex ω plane that also satisfies $\mathrm{Im}[H(\omega)] \geq 0$ for $\mathrm{Im}(\omega) > 0$ [2,22]. Based on the different descriptions of passivity mentioned above, two types of Herglotz functions can be introduced for the unidimensional scattering problem. For the admittance/impedance passivity equation (2.4), we define

$$H_1(\omega) = \mathrm{i}\eta(\omega) \tag{2.6a}$$

or

$$H_1(\omega) = \mathrm{i}\zeta(\omega). \tag{2.6b}$$

Analogously, for the scattering passivity in equation (2.5), the Herglotz functions can be defined as follows:

$$H_2(\omega) = -\mathrm{i}\log[R(\omega)B(\omega)] \tag{2.7a}$$

or

$$H_2(\omega) = -\mathrm{i}\log[T(\omega)B(\omega)], \tag{2.7b}$$

where log(·) is the complex logarithm, in contrast to the natural logarithm ln(·), which stands for real variables. $B(\omega)$ is a Blaschke product introduced to remove the zeros of $R(\omega)$ or $T(\omega)$ (i.e. the singularities of the corresponding complex logarithm) from the upper half complex ω plane [2,16–18]. The Blaschke product is defined as follows:

$$B(\omega) = \prod_n \frac{1 - \omega/\omega_n^*}{1 - \omega/\omega_n}, \tag{2.8}$$

where ω_n is the nth zero of $R(\omega)$ or $T(\omega)$ in equations (2.7) with $\mathrm{Im}(\omega_n) > 0$ and the star denotes the complex conjugate. Note that $-B(\omega)$ can be used instead of $B(\omega)$ when the soft-boundary reflection problem is considered. Also note that we will use different Herglotz functions for each passivity condition, i.e. either the form (a) or (b) in equations (2.6) and (2.7), depending on their static and dynamic limits.

When the input/output functions are real-valued in the time domain, the Herglotz functions introduced in equations (2.6) and (2.7) are symmetric, i.e. $H(\omega) = -H^*(-\omega^*)$ is satisfied. From the representation theorem [2], the asymptotic expansions of a symmetric Herglotz function in the static limit ($\omega \hat{\to} 0$) and the dynamic limit ($\omega \hat{\to} \infty$) can be written as

$$H(\omega) = \frac{a_{-1}}{\omega} + a_1\omega + \cdots + a_{2N_0-1}\omega^{2N_0-1} + o(\omega^{2N_0-1}), \quad \text{when } \omega \hat{\to} 0 \tag{2.9a}$$

and

$$H(\omega) = b_1\omega + \frac{b_{-1}}{\omega} + \cdots + \frac{b_{1-2N_\infty}}{\omega^{2N_\infty-1}} + o\left(\frac{1}{\omega^{2N_\infty-1}}\right), \quad \text{when } \omega \hat{\to} \infty, \tag{2.9b}$$

where a_n, b_n are real coefficients, and N_0, N_∞ are non-negative integers. Moreover, the expansions should be stopped whenever a term that does not satisfy the forms of equations (2.9) appears (e.g. $\log\omega$, $\sqrt{\omega}$, constant or any even-order term of ω). Note that the notation $\hat{\to}$ denotes the limit in the Stoltz domain $\theta \le \arg\omega \le \pi - \theta$, for any $0 < \theta \le \pi/2$, in the complex ω plane rather than on the real axis. As shown in [2], the coefficients a_n and b_n in equations (2.9) can then be used to construct a series of integral identities or sum rules

$$\lim_{\varepsilon\to 0^+}\lim_{\delta\to 0^+}\frac{2}{\pi}\int_\varepsilon^{\varepsilon^{-1}}\frac{\mathrm{Im}[H(\omega+\mathrm{i}\delta)]}{\omega^{2n}}\,\mathrm{d}\omega = a_{2n-1} - b_{2n-1}, \tag{2.10}$$

where $n = 1 - N_\infty, \ldots, N_0$. Note that not every symmetric Herglotz function does admit a sum rule. A trivial example is that $H(\omega) = \mathrm{i}C$, where $C > 0$. It is easy to validate that $H(\omega)$ is a symmetric Herglotz function; however, the leading terms of its asymptotic expansions are a_0 and b_0 terms, with which the general formula (2.10) is not applicable.

In each case considered in this work, the $n = 1$ sum rule is allowed. We have thus

$$\frac{2}{\pi}\int_0^\infty \frac{\mathrm{Im}[H(\omega)]}{\omega^2}\,\mathrm{d}\omega = a_1 - b_1, \tag{2.11}$$

in which the integral from zero to infinity is a shorthand notation for the limits in equation (2.10). In the following sections, we will show that the diverging term $b_1\omega$ in the dynamic limit does not exist in most cases, i.e. $b_1 = 0$, so that the $n = 1$ sum rule only involves the static limit of the system. The only exception is the sum rule for $T(\omega)$ in the transmission problem. In this case, b_1, which represents the group delay [43] induced by the material layer, does not vanish. Hence, this particular sum rule is influenced by both the static and dynamic limits of the system.

3. Fundamental constraints for unidimensional scattering problems

(a) Transfer matrix modelling of the system

We consider several unidimensional scattering problems in which an incident plane wave is scattered by an effective material with thickness L as illustrated in figure 1. We assume that this material consists of rigid, motionless and subwavelength elements, e.g. tubes, cavities, perforations, porous materials, etc. Note that these elements are not restricted to be merely inside

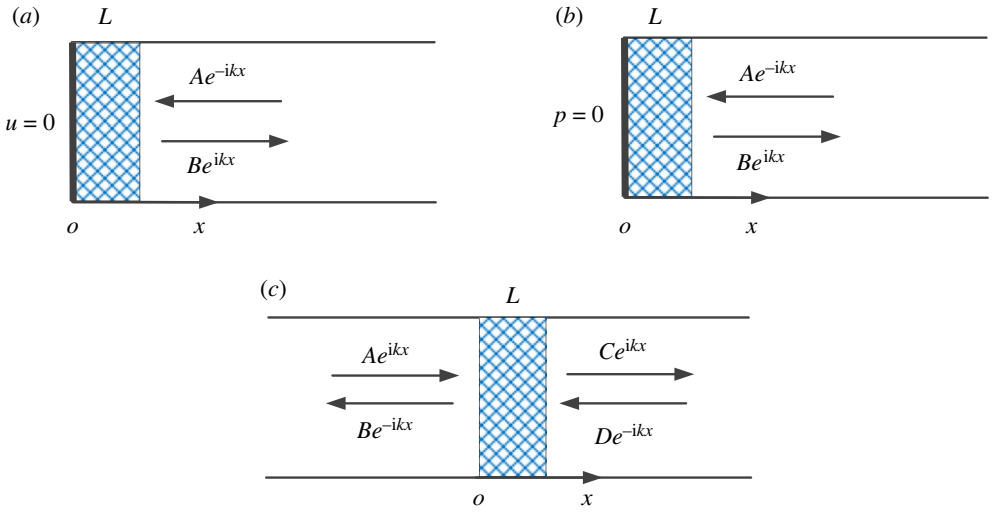

Figure 1. The unidimensional scattering problem of a plane wave by a mirror-symmetric effective material: (*a*) rigid-boundary reflection problem, (*b*) soft-boundary reflection problem and (*c*) transmission problem. (Online version in colour.)

the waveguide. Side branch elements could also be accounted for in this effective layer through the homogenization theory [39,40]. All the elements as well as the waveguide are saturated by air with density ρ_0 and adiabatic sound speed c_0. The losses within the system are induced by viscothermal boundary layers near the no-slip and isothermal boundaries.

We start from the case in which the effective material is mirror symmetric, so that the acoustic behaviour of the material can be modelled as an equivalent fluid layer with frequency-dependent effective parameters [39–41]. This configuration is subsequently generalized to account for multilayer structures that are locally mirror symmetric (each sublayer is mirror symmetric).

Under the above assumptions, the state vector at $x = L$ can be related to that at $x = 0$ through the transfer matrix $\mathbf{T}$ of the single-layer system [39,40]:

$$\begin{bmatrix} P(L) \\ U(L) \end{bmatrix} = \mathbf{T} \begin{bmatrix} P(0) \\ U(0) \end{bmatrix} = \begin{bmatrix} t_{11} & t_{12} \\ t_{21} & t_{22} \end{bmatrix} \begin{bmatrix} P(0) \\ U(0) \end{bmatrix}, \tag{3.1}$$

where $P = p/K_0$, $U = u/c_0$ refer to the dimensionless forms of acoustic pressure and particle velocity: the acoustic pressure p and particle velocity u are normalized by the adiabatic bulk modulus $K_0 = \rho_0 c_0^2$ and the sound speed c_0 of air, respectively. The elements of the transfer matrix are

$$t_{11} = t_{22} = \cos(k_e L), \tag{3.2a}$$

$$t_{12} = \mathrm{i}\frac{z_e}{z_0}\sin(k_e L) \tag{3.2b}$$

and

$$t_{21} = \mathrm{i}\frac{z_0}{z_e}\sin(k_e L), \tag{3.2c}$$

in which $z_0 = \rho_0 c_0$ refers to the characteristic impedance of air. The effective parameters of the material are frequency-dependent, including its density ρ_e, sound speed c_e, characteristic impedance $z_e = \rho_e c_e$ and acoustic wavenumber $k_e = \omega/c_e$. The static and dynamic limits of these parameters can be rigorously evaluated [41]; details are provided in appendix A. Either for the unidimensional reflection problems or the unidimensional transmission problem, the acoustical response functions of the system can be expressed in terms of the elements of the transfer matrix.

(b) Rigid-boundary reflection problem

We first consider the reflection problem shown in figure 1*a* where a rigid boundary ($u = 0$) is imposed at one end of the material ($x = 0$). In this case, the relevant response functions are the surface admittance and the reflection coefficient at $x = L$. They are given by

$$\eta(\omega) = -\frac{t_{21}}{t_{11}} = -\mathrm{i}\frac{z_0}{z_e}\tan(k_e L) \tag{3.3a}$$

and

$$R(\omega) = \frac{t_{11} + t_{21}}{t_{11} - t_{21}} = \frac{z_e + \mathrm{i}z_0\tan(k_e L)}{z_e - \mathrm{i}z_0\tan(k_e L)}. \tag{3.3b}$$

With the choice of Herglotz functions H_1 and H_2 defined in equation (2.6*a*) and equation (2.7*a*), together with the Blaschke product B from equation (2.8), the following $n = 1$ sum rules (as shown in equation (2.11)) can be derived for η and R

$$\frac{2c_0}{\pi}\frac{K_e(0)}{K_0}\int_0^\infty \frac{1}{\omega^2}\mathrm{Re}[\eta(\omega)]\,\mathrm{d}\omega = L \tag{3.4a}$$

and

$$\frac{c_0}{\pi}\frac{K_e(0)}{K_0}\int_0^\infty \frac{-1}{\omega^2}\ln|R(\omega)|\,\mathrm{d}\omega \le L. \tag{3.4b}$$

The first sum rule (3.4*a*) implies that when the thickness of a passive treatment is fixed, the resistance cannot be an arbitrarily chosen function of frequency. The second sum rule (3.4*b*) is an inequality because the static limit of the Blaschke product is dropped in the expansion of the Herglotz function (i.e. in the a_1 term), as explained in appendix B. Besides, equation (3.4*b*) can be rearranged as a sum rule for the weighted absorption spectrum, due to the relation $\alpha(\omega) = 1 - |R(\omega)|^2$

$$\frac{c_0}{2\pi}\frac{K_e(0)}{K_0}\int_0^\infty \frac{-1}{\omega^2}\ln[1-\alpha(\omega)]\,\mathrm{d}\omega \le L. \tag{3.5}$$

The sum rules (3.4*a*)–(3.5) are clearly controlled by the effective bulk modulus of the material $K_e = \rho_e c_e^2$, which is expected since the low-frequency response of the system is monopolar (see [44–46] and ch. 5 of [40]). The static limit of K_e can be derived as (see appendix A, or p. 56 in [41])

$$\frac{K_e(0)}{K_0} = \frac{1}{\gamma\phi}, \tag{3.6}$$

where $\gamma = 1.4$ is the adiabatic index of air and ϕ is defined as the volume ratio between the saturating air and the whole layer. When all the elements of the material are fixed inside the waveguide, ϕ is the porosity of the material and $\phi \le 1$ is well satisfied. In the opposite, when side-branch elements are also included, ϕ could be larger than unity, because the volume of the the effective layer could be less than that of the material. The inequality (3.5) is in accordance with the results given in [18,27], which provide a design criterion for the minimum total length of a broadband absorber. However, a difference exists in the evaluation of $K_e(0)$. In [18], the system is modelled as a Lorentz oscillator, so that the losses are independent of frequency. As a result, the static limit of the effective bulk modulus tends to the adiabatic limit, which leads to $K_e(0)/K_0 = 1/\phi$ (shown in [18]). Conversely, the viscothermal losses in the system are considered here by introducing frequency-dependent effective parameters in the transfer matrix. As a consequence, the effective bulk modulus tends to the isothermal limit, which leads to the additional factor γ in equation (3.6).

From a practical point of view, the sum rule (3.5) can be used to provide guidelines for the design of acoustic treatments. For instance, if the aim is to achieve an absorption target $\alpha(\omega)$ then equation (3.5) provides a lower bound for the quantity $LK_0/K_e(0)$. Since the porosity of the treatment can be estimated before a specific design, it is then possible to identify the minimum length $L_{\min}$ of the treatment to meet this absorption target. An example is provided in §4. Alternatively, for a given treatment with thickness L and static limit $K_e(0)$, equation (3.5) indicates the levels of the absorption spectrum that can be achieved with this treatment. Furthermore, the

importance of the $1/\omega^2$ weighting terms in equation (3.5) should be emphasized. It implies that absorbing lower frequencies will require increasingly larger treatments. In other words, if the target absorption α is close to one at low frequencies, $L_{\min}$ will be particularly large.

The above sum rules are readily extended to the case of a multilayer composite material. In the static limit, the effective bulk modulus of the stratified medium can be obtained from those of the individual layers via a first-order homogenization scheme [39,40]. This analysis directly results in the following sum rules:

$$\frac{2c_0}{\pi}\int_0^\infty \frac{1}{\omega^2}\mathrm{Re}[\eta(\omega)]\,\mathrm{d}\omega = \sum_i \left[\frac{K_0}{K_{e,i}(0)}L_i\right], \tag{3.7a}$$

$$\frac{c_0}{\pi}\int_0^\infty \frac{-1}{\omega^2}\ln|R(\omega)|\,\mathrm{d}\omega \le \sum_i \left[\frac{K_0}{K_{e,i}(0)}L_i\right] \tag{3.7b}$$

and

$$\frac{c_0}{2\pi}\int_0^\infty \frac{-1}{\omega^2}\ln[1-\alpha(\omega)]\,\mathrm{d}\omega \le \sum_i \left[\frac{K_0}{K_{e,i}(0)}L_i\right], \tag{3.7c}$$

in which $K_{e,i}$, L_i are the effective bulk modulus and length of the ith layer, respectively. With equation (3.6), the right-hand sides of equations (3.7) can be further evaluated as

$$\sum_i \left[\frac{K_0}{K_{e,i}(0)}L_i\right] \le \gamma\phi_{\max}L, \tag{3.8}$$

where $\phi_{\max}$ is the maximum air filling ratio among all the layers, and $L=\sum_i L_i$ is the total length of the material.

(c) Soft-boundary reflection problem

We now consider the reflection problem depicted in figure 1*b* where a pressure-release boundary condition ($p=0$) is used at $x=0$. The relevant response functions are then

$$\zeta(\omega) = -\frac{t_{12}}{t_{22}} = -\mathrm{i}\frac{z_e}{z_0}\tan(k_eL) \quad \text{or} \quad \eta(\omega) = -\frac{t_{22}}{t_{12}} = \mathrm{i}\frac{z_0}{z_e}\cot(k_eL) \tag{3.9a}$$

and

$$R(\omega) = \frac{t_{12}+t_{22}}{t_{12}-t_{22}} = \frac{z_e - \mathrm{i}z_0\cot(k_eL)}{z_e+\mathrm{i}z_0\cot(k_eL)}. \tag{3.9b}$$

In contrast to the rigid-boundary reflection problem, the static limits of ζ, η and R depend on the normalized steady flow resistance of the layer (see appendix B for the derivation), defined by

$$\xi = \frac{L\sigma}{z_0}, \tag{3.10}$$

where σ is the steady flow resistivity and $L\sigma$ measures the pressure loss caused by a low-speed steady flow across the layer. When in-series elements within the waveguide are considered, the steady flow resistivity can be expressed by $\sigma=(C_1\mu_0)/(r_H^2\phi)$. The positive real constant C_1 is determined by the geometry of the elements of the material, e.g. for a circular tube $C_1=8$ while for a two-dimensional slit $C_1=3$ (see pp. 58–59 in [41]). The dynamic viscosity of air is denoted μ_0 and $r_H=2\bar{A}_c/\bar{P}_c$ is a typical length scale of the elements. $\bar{A}_c$ and $\bar{P}_c$ represent the averaged values of the area and perimeter of the cross sections of all the elements of the material, respectively. When all these have identical cross sections, r_H is one-half of the hydraulic diameter (e.g. r_H is the radius for a circular cross section) and is then the half-width of a two-dimensional slit.

The $n=1$ sum rule (2.11) is applicable only when the layer is either non-resistive ($\xi\to 0$) or highly resistive ($\xi\to\infty$). Apart from these two cases, the Herglotz functions H_1 and H_2 approach to constants in the static and dynamic limits (i.e. a_0 and b_0 are the leading order terms in the asymptotic expansions as shown in appendix B), and thus, no sum rule is available. However, it is still worth mentioning that, in the special case that the steady flow resistance of the layer matches the characteristic impedance of air (i.e. $\xi=1$), the static limit of the reflection coefficient

vanishes, i.e. $R(0) = 0$ (see the asymptotic expansion of $R(\omega)$ in appendix B). In other words, the specific length $L = z_0/\sigma$ leads to perfect absorption in the static limit for any given material. This feature of soft-boundary reflection problem enables designs of space-saving absorbers in the ultra-low-frequency range. In [47], a specific design has been proposed and validated experimentally.

In the next two subsections, we focus on the two distinct cases $\xi \to 0$ and $\xi \to \infty$ in which sum rules of the system are available. When the layer is non-resistive ($\xi \to 0$), the static limit $R(0) = -1$, and the response of the system is of dipolar nature [40,44–46]. In the opposite, when the layer is highly resistive ($\xi \to \infty$), $R(0) = 1$ and a monopolar-type response is recovered.

(i) Non-resistive material: $\xi \to 0$

First, we consider a non-resistive material. In contrast to the rigid-boundary reflection problem, the impedance ζ is used to construct the Herglotz function H_1 in equation (2.6*b*) because $\zeta(0) = O(\omega)$ in the static limit, which provides the a_1 term for the $n = 1$ sum rule, whereas $\eta(0)$ blows up. The Herglotz function H_2 is built from equation (2.7*a*) with the reflection coefficient R and the Blaschke product $-B$ instead of B. These Herglotz functions H_1 and H_2 lead to the following sum rules:

$$\frac{2c_0}{\pi}\frac{\rho_0}{\mathrm{Re}[\rho_e(0)]}\int_0^\infty \frac{1}{\omega^2}\mathrm{Re}[\zeta(\omega)]\,\mathrm{d}\omega = L \tag{3.11a}$$

and

$$\frac{c_0}{\pi}\frac{\rho_0}{\mathrm{Re}[\rho_e(0)]}\int_0^\infty \frac{-1}{\omega^2}\ln|R(\omega)|\,\mathrm{d}\omega \le L. \tag{3.11b}$$

Moreover, equation (3.11*b*) can be rearranged to obtain a sum rule for the absorption coefficient

$$\frac{c_0}{2\pi}\frac{\rho_0}{\mathrm{Re}[\rho_e(0)]}\int_0^\infty \frac{-1}{\omega^2}\ln[1-\alpha(\omega)]\,\mathrm{d}\omega \le L. \tag{3.12}$$

Due to the dipolar nature of the system, the real part of the effective density, $\mathrm{Re}(\rho_e)$, controls the above sum rules. Its static limit is given by

$$\frac{\mathrm{Re}[\rho_e(0)]}{\rho_0} = \frac{C_2}{\phi}, \tag{3.13}$$

where the positive real constant C_2 depends on the cross-sectional geometry of the components of the material. When a material composed of in-series elements along the waveguide is considered, C_2 varies between 1.2 and 1.44 for commonly used shapes (see p. 64 in [41]).

The sum rules equations (3.11) and (3.12) can be generalized to a multilayer material through the homogenization theory [39,40], which yields

$$\frac{2c_0}{\pi}\int_0^\infty \frac{1}{\omega^2}\mathrm{Re}[\zeta(\omega)]\,\mathrm{d}\omega = \sum_i \left\{\frac{\mathrm{Re}[\rho_{e,i}(0)]}{\rho_0}L_i\right\}, \tag{3.14a}$$

$$\frac{c_0}{\pi}\int_0^\infty \frac{-1}{\omega^2}\ln|R(\omega)|\,\mathrm{d}\omega \le \sum_i \left\{\frac{\mathrm{Re}[\rho_{e,i}(0)]}{\rho_0}L_i\right\} \tag{3.14b}$$

and

$$\frac{c_0}{2\pi}\int_0^\infty \frac{-1}{\omega^2}\ln[1-\alpha(\omega)]\,\mathrm{d}\omega \le \sum_i \left\{\frac{\mathrm{Re}[\rho_{e,i}(0)]}{\rho_0}L_i\right\}, \tag{3.14c}$$

where $\rho_{e,i}$ is the effective density of the i-th layer with length L_i. With equation (3.13), the right-hand sides of equations (3.14) can be written as

$$\sum_i \left\{\frac{\mathrm{Re}[\rho_{e,i}(0)]}{\rho_0}L_i\right\} \le L\left(\frac{C_2}{\phi}\right)_{\max}, \tag{3.15}$$

which indicates that, to involve the total length $L = \sum_i L_i$ in the sum rules (3.14) explicitly, the maximum value of C_2/ϕ among all the layers should be evaluated.

(ii) Highly resistive material: $\xi \to \infty$

Second, a highly resistive material is considered. Similarly to the reflection problem with a rigid wall, the surface admittance η and reflection coefficient R are the relevant response functions. Correspondingly, the Herglotz functions H_1 and H_2 from equation (2.6*a*) and equation (2.7*a*) with Blaschke product B in equation (2.8) are employed to yield the following $n=1$ sum rules:

$$\frac{6c_0}{\pi}\frac{K_e(0)}{K_0}\int_0^\infty \frac{1}{\omega^2}\mathrm{Re}[\eta(\omega)]\,\mathrm{d}\omega = L \tag{3.16a}$$

and

$$\frac{3c_0}{\pi}\frac{K_e(0)}{K_0}\int_0^\infty \frac{-1}{\omega^2}\ln|R(\omega)|\,\mathrm{d}\omega \le L. \tag{3.16b}$$

The corresponding sum rule for the absorption coefficient is

$$\frac{3c_0}{2\pi}\frac{K_e(0)}{K_0}\int_0^\infty \frac{-1}{\omega^2}\ln[1-\alpha(\omega)]\,\mathrm{d}\omega \le L. \tag{3.17}$$

Note that the coefficients on the left-hand sides of equations (3.16) and (3.17) are three times larger than those in the sum rules in equations (3.4) and (3.5). This factor three arises from the first-order terms in ω in the low-frequency expansions of $\tan(k_eL)/z_e$ in the rigid-boundary reflection problem and of $\cot(k_eL)/z_e$ in the soft-boundary reflection problem, respectively (see equations (3.3) and (3.9)). They are thus intrinsically related to the boundary condition, either rigid wall or pressure release boundary conditions.

For the multilayer case, the above sum rules can be generalized to

$$\frac{6c_0}{\pi}\int_0^\infty \frac{1}{\omega^2}\mathrm{Re}[\eta(\omega)]\,\mathrm{d}\omega = \sum_i\left[\frac{K_0}{K_{e,i}(0)}L_i\right], \tag{3.18a}$$

$$\frac{3c_0}{\pi}\int_0^\infty \frac{-1}{\omega^2}\ln|R(\omega)|\,\mathrm{d}\omega \le \sum_i\left[\frac{K_0}{K_{e,i}(0)}L_i\right] \tag{3.18b}$$

and

$$\frac{3c_0}{2\pi}\int_0^\infty \frac{-1}{\omega^2}\ln[1-\alpha(\omega)]\,\mathrm{d}\omega \le \sum_i\left[\frac{K_0}{K_{e,i}(0)}L_i\right], \tag{3.18c}$$

where $K_{e,i}$ is the effective bulk modulus of the ith layer with length L_i. Similarly to the rigid-boundary reflection problem, the right-hand sides of equations (3.18) could be evaluated by equation (3.8).

(d) Transmission problem

For a non-reciprocal and asymmetric system, the reflection and transmission coefficients in the transmission problem are given by

$$R^-(\omega) = \frac{-t_{11}-t_{12}+t_{21}+t_{22}}{t_{11}-t_{12}-t_{21}+t_{22}} = \frac{\mathrm{i}\tan(k_eL)[(z_0/z_e)-(z_e/z_0)]}{2-\mathrm{i}\tan(k_eL)[(z_0/z_e)+(z_e/z_0)]}, \tag{3.19a}$$

$$T^-(\omega) = \frac{2\mathrm{e}^{-\mathrm{i}k_0L}(t_{11}t_{22}-t_{12}t_{21})}{t_{11}-t_{12}-t_{21}+t_{22}} = \frac{2\mathrm{e}^{-\mathrm{i}k_0L}}{2\cos(k_eL)-\mathrm{i}\sin(k_eL)[(z_0/z_e)+(z_e/z_0)]}, \tag{3.19b}$$

$$R^+(\omega) = \frac{t_{11}-t_{12}+t_{21}-t_{22}}{t_{11}-t_{12}-t_{21}+t_{22}} = \frac{\mathrm{i}\tan(k_eL)[(z_0/z_e)-(z_e/z_0)]}{2-\mathrm{i}\tan(k_eL)[(z_0/z_e)+(z_e/z_0)]} \tag{3.19c}$$

and

$$T^+(\omega) = \frac{2\mathrm{e}^{-\mathrm{i}k_0L}}{t_{11}-t_{12}-t_{21}+t_{22}} = \frac{2\mathrm{e}^{-\mathrm{i}k_0L}}{2\cos(k_eL)-\mathrm{i}\sin(k_eL)[(z_0/z_e)+(z_e/z_0)]}, \tag{3.19d}$$

in which the superscripts $^-$ and $^+$ refer to the surface $x=0$ and $x=L$, respectively. In the case shown in figure 1*c*, we consider a reciprocal system, $t_{11}t_{22}-t_{12}t_{21}=1$ and thus $T^-(\omega)=T^+(\omega)\equiv T(\omega)$. Moreover, for a mirror symmetric single layer, $R^-(\omega)=R^+(\omega)\equiv R(\omega)$, i.e. $t_{11}=t_{22}$. Similarly to the soft-boundary reflection problem, the static limits of both $T(\omega)$ and $R(\omega)$ depend on the steady flow resistance ξ.

When the material is non-resistive ($\xi \to 0$), $T(0) = 1$ and $R(0) = 0$. As a result, the $n = 1$ sum rule (2.11) is available only for Herglotz functions constructed from the transmission coefficient $T(\omega)$. By contrast, when the material is highly resistive ($\xi \to \infty$), $T(0) = 0$ and $R(0) = 1$. Consequently, the sum rules with the reflection coefficient $R(\omega)$ can be derived from equation (2.11). Similarly to the soft-boundary reflection problem, in other cases when ξ possesses the moderate values, the Herglotz functions H_1 and H_2 do not lead to sum rules. However, in the special case where $\xi = 2$, $R(0) = T(0) = 1/2$, so that the absorption coefficient, defined by $\alpha = 1 - |R|^2 - |T|^2$, reaches its maximum value in the static limit, i.e. $\alpha = 1/2$. Note that the maximum absorption coefficient of a point scatterer in the transmission problem is $1/2$ at any frequency. Proofs are given in [44,46].

(i) Non-resistive material: $\xi \to 0$

We first consider the case of a non-resistive material, $\xi \to 0$. By an analogy with the surface admittance in the reflection problem, a bilinear transformation, which maps the unit disc to the closed upper half plane (see p. 131 in [48]), is used to construct the Herglotz function H_1 with the transmission coefficient

$$H_1(\omega) = \mathrm{i}\frac{1 - T(\omega)}{1 + T(\omega)}. \tag{3.20}$$

The other Herglotz function, H_2, is derived from equation (2.7*b*), with the Blaschke product B in equation (2.8). It follows that the corresponding sum rules are

$$\frac{8c_0}{\pi}\left\{\frac{K_0}{K_e(0)} + \frac{\mathrm{Re}[\rho_e(0)]}{\rho_0} - 2\right\}^{-1}\int_0^\infty \frac{1}{\omega^2}\mathrm{Re}\left[\frac{1 - T(\omega)}{1 + T(\omega)}\right]\mathrm{d}\omega = L \tag{3.21a}$$

and

$$\frac{4c_0}{\pi}\left\{\frac{K_0}{K_e(0)} + \frac{\mathrm{Re}[\rho_e(0)]}{\rho_0} - 2\frac{c_0}{c_\infty}\right\}^{-1}\int_0^\infty \frac{-1}{\omega^2}\ln|T(\omega)|\,\mathrm{d}\omega \le L. \tag{3.21b}$$

In the static limit, the layer of composite material reduces to a point scatterer and thus the transmission problem can be interpreted as a linear combination of a monopolar- and a dipolar-type reflection problems [40,44–46,49]. As a consequence, both the effective bulk modulus and the effective density are involved in equations (3.21). Note that the dynamic behaviour of the system contributes to the second sum rule (3.21*b*). c_∞ refers to the dynamic limit of the effective sound speed, and can be evaluated by

$$\frac{c_\infty}{c_0} = \frac{1}{\sqrt{\tau_\infty}}, \tag{3.22}$$

where $\tau_\infty \ge 1$ is the tortuosity of the material (see p. 67 of [41]). According to equations (3.6) and (3.13),

$$\frac{K_0}{K_e(0)} + \frac{\mathrm{Re}[\rho_e(0)]}{\rho_0} = \gamma\phi + \frac{C_2}{\phi}. \tag{3.23}$$

For any $\phi \ge 0$, it can be found that $\gamma\phi + C_2/\phi \ge 2\sqrt{\gamma C_2}$. In [50] and p. 82 of [41], C_2 is alternatively denoted as the static tortuosity, τ_0, of the material. Moreover, according to [51], $\tau_0 \ge \tau_\infty$. Therefore, $\gamma\phi + C_2/\phi \ge 2\sqrt{\gamma\tau_\infty} > 2\sqrt{\tau_\infty}$, and it follows that

$$\frac{K_0}{K_e(0)} + \frac{\mathrm{Re}[\rho_e(0)]}{\rho_0} > 2\frac{c_0}{c_\infty} > 2, \tag{3.24}$$

which ensures that the left-hand sides of equations (3.21) are positive. When the tortuosity τ_∞ is hard to evaluate before a specific design, $\tau_\infty = 1$ could be used, which results in a lower bound of L when applying the sum rule (3.21*b*).

To obtain the constraints on the transmission loss and the absorption coefficient, the relations $\mathrm{TL}(\omega) = -20\log_{10}|T(\omega)|$ and $1 - \alpha(\omega) = |T(\omega)|^2 + |R(\omega)|^2 \ge |T(\omega)|^2$ can be combined with

equation (3.21*b*) to write

$$\frac{c_0 \ln 10}{5\pi}\left\{\frac{K_0}{K_e(0)}+\frac{\mathrm{Re}[\rho_e(0)]}{\rho_0}-2\frac{c_0}{c_\infty}\right\}^{-1}\int_0^\infty \frac{\mathrm{TL}(\omega)}{\omega^2}\,\mathrm{d}\omega \le L \tag{3.25a}$$

and

$$\frac{2c_0}{\pi}\left\{\frac{K_0}{K_e(0)}+\frac{\mathrm{Re}[\rho_e(0)]}{\rho_0}-2\frac{c_0}{c_\infty}\right\}^{-1}\int_0^\infty \frac{-1}{\omega^2}\ln[1-\alpha(\omega)]\,\mathrm{d}\omega \le L. \tag{3.25b}$$

We then consider a multilayer material. The reciprocity of the system still holds, so that $T^-(\omega)=T^+(\omega)$, but this system can then become asymmetric and consequently $R^-(\omega)$ and $R^+(\omega)$ might be different. In the low-frequency regime, the asymmetric part can be modelled by introducing the Willis coupling constant [52–54], when the homogenization method is applied. The coupling constant appears as a second-order term of ω, and thus, the system falls back to a symmetric one in the static limit. However, the dynamic limit has to be derived from the transfer matrix of the entire system. These considerations provide a generalization of the sum rules in equations (3.21) and (3.25)

$$\frac{8c_0}{\pi}\int_0^\infty \frac{1}{\omega^2}\mathrm{Re}\left[\frac{1-T(\omega)}{1+T(\omega)}\right]\mathrm{d}\omega=\sum_i L_i\left\{\frac{K_0}{K_{e,i}(0)}+\frac{\mathrm{Re}[\rho_{e,i}(0)]}{\rho_0}-2\right\}, \tag{3.26a}$$

$$\frac{4c_0}{\pi}\int_0^\infty \frac{-1}{\omega^2}\ln|T(\omega)|\,\mathrm{d}\omega \le \sum_i L_i\left\{\frac{K_0}{K_{e,i}(0)}+\frac{\mathrm{Re}[\rho_{e,i}(0)]}{\rho_0}-2\frac{c_0}{c_{\infty,i}}\right\}, \tag{3.26b}$$

$$\frac{c_0 \ln 10}{5\pi}\int_0^\infty \frac{\mathrm{TL}(\omega)}{\omega^2}\,\mathrm{d}\omega \le \sum_i L_i\left\{\frac{K_0}{K_{e,i}(0)}+\frac{\mathrm{Re}[\rho_{e,i}(0)]}{\rho_0}-2\frac{c_0}{c_{\infty,i}}\right\} \tag{3.26c}$$

and

$$\frac{2c_0}{\pi}\int_0^\infty \frac{-1}{\omega^2}\ln[1-\alpha(\omega)]\,\mathrm{d}\omega \le \sum_i L_i\left\{\frac{K_0}{K_{e,i}(0)}+\frac{\mathrm{Re}[\rho_{e,i}(0)]}{\rho_0}-2\frac{c_0}{c_{\infty,i}}\right\}, \tag{3.26d}$$

in which $K_{e,i}$, $\rho_{e,i}$ are the effective bulk modulus and density, respectively, $c_{\infty,i}$ denotes the dynamic limit of the effective sound speed of the ith layer with length L_i. Note that

$$\sum_i L_i\left\{\frac{K_0}{K_{e,i}(0)}+\frac{\mathrm{Re}[\rho_{e,i}(0)]}{\rho_0}-2\right\} \le L\left(\gamma\phi+\frac{C_2}{\phi}-2\right)_{\max} \tag{3.27}$$

and

$$\sum_i L_i\left\{\frac{K_0}{K_{e,i}(0)}+\frac{\mathrm{Re}[\rho_{e,i}(0)]}{\rho_0}-2\frac{c_0}{c_{\infty,i}}\right\} \le L\left(\gamma\phi+\frac{C_2}{\phi}-2\sqrt{\tau_\infty}\right)_{\max}, \tag{3.28}$$

where $L=\sum_i L_i$ is the total length of the material.

(ii) Highly resistive material: $\xi \to \infty$

For the transmission problem with a highly resistive material, the relevant response functions are the surface admittance

$$\eta^{\pm}(\omega)=\frac{1-R^{\pm}(\omega)}{1+R^{\pm}(\omega)}, \tag{3.29}$$

and the reflection coefficients $R^{\pm}(\omega)$. Since the material is considered mirror symmetric, both η and R are identical on either side. It follows that the Herglotz functions H_1 and H_2 are defined in equations (2.6*a*) and (2.7*a*) with the Blaschke product in equation (2.8).

It is found that the sum rules in this situation take exactly the same form as in equations (3.16) and (3.17) in the soft-boundary reflection problem. The details of the asymptotic expansions of H_1 and H_2 are available in appendix B. A multilayer generalization directly results in sum rules expressed by equations (3.18), considering that the multilayer material still has the mirror symmetry in the static limit because the Willis material falls back to be symmetric.

4. Applications of the sum rules

The derived sum rules relate the target spectrum of the relevant response functions to the static/dynamic limits of the equivalent parameters as well as the total length of the layer (or the length of each layer). Thus, the required minimum total length of the treatment can be predicted before any specific design provided these limits are well predicted by *a priori* estimates on the porosity and the tortuosity. Two specific examples are given in this section to show the practical applications of the sum rules.

The first example deals with the sum rule of a broadband absorber in the rigid-boundary reflection problem: when a target absorption spectrum is provided, the sum rule can be used to evaluate the required minimum length of the absorber. Apart from the rigid-boundary reflection problem, all the sum rules derived in the soft-boundary reflection problem and the transmission problem depend on the steady flow resistance $\xi = L\sigma/z_0$. Therefore, an estimation of ξ should be made to select the suitable sum rule. After the prediction of the minimum length, the value of ξ should be examined. However, some cases exist for which ξ can be easily fixed. These cases are of great importance in practical applications as well. The second example of this section focuses on the transmission problem of a ring-shaped muffler in parallel of the circular waveguide with grazing incident wave. When the viscothermal losses in the main duct can be neglected compared with those induced by the muffler, this scenario provides a case for which the effective layer is perfectly non-resistive, i.e. $\xi = 0$. It is shown that, when a target transmission loss spectrum is provided, the required minimum volume of the muffler can be predicted by the sum rule.

It should be noted that due to the weighting factor $1/\omega^2$ in all the derived sum rules, the low-frequency spectrum of the target response function has a dramatic effect on the predicted total length of the system. However, without a specific design, there is usually a lack of details on the target function near the static limit. In both of the following examples, we fix this problem by interpolating the target spectra, in which the basis functions are properly chosen to preserve the asymptotic behaviours of the corresponding target functions in the static limit.

(a) Minimum length of a broadband absorber for a target absorption spectrum in the rigid-boundary reflection problem

As illustrated in figure 1*a*, we assume that the layer of material is composed of in-series elements or laminates fixed within the waveguide. According to the sum rule (3.5), the minimum length can be predicted by

$$L_{\min} = \frac{-c_0}{4\pi^2\gamma\phi}\int_{f_1}^{f_2}\frac{\ln[1-\alpha_T(f)]}{f^2}\,\mathrm{d}f, \tag{4.1}$$

where α_T is the target spectrum, given within the frequency range $[f_1, f_2]$. From equation (4.1), it is clear that the integral blows up if we choose $\alpha_T = 1$ from f_1 to f_2. This implies that, in principle, broadband-perfect absorption cannot be realized by an absorber with finite length. In fact, if perfect absorption is achieved in a finite frequency range, $\alpha = 1$ is guaranteed at any frequency. Provided that the reflection coefficient $R(\omega)$ is a constant zero within a finite interval, then $R(\omega)$ equals the same constant in the whole complex ω plane, due to the Cauchy–Riemann conditions [48,55] satisfied by real and imaginary parts of a holomorphic function. However, this does not prevent perfect absorption occurring at discrete frequencies. Moreover, when perfect absorption is achieved, α should be less than unity in the bands between these discrete frequencies [28].

In practical applications, the target spectrum is usually presented in octave bands or 1/3 octave bands. By contrast, a simplified target spectrum is employed here. We assume that the absorption coefficient is larger than 0.3, 0.6 and 0.9 at 100 Hz, 500 Hz and 2500 Hz, respectively. According to equation (4.1), it seems that the most efficient absorber (which has the minimum length) is achieved when α_T is exactly zero outside the considered frequency band. However, this idealized target spectrum is not physically accessible. Particularly, the absorption coefficient possesses the quadratic nature in the low-frequency range [27], i.e. $\alpha \sim (k_0 L)^2$. Thus, in this case, we assume

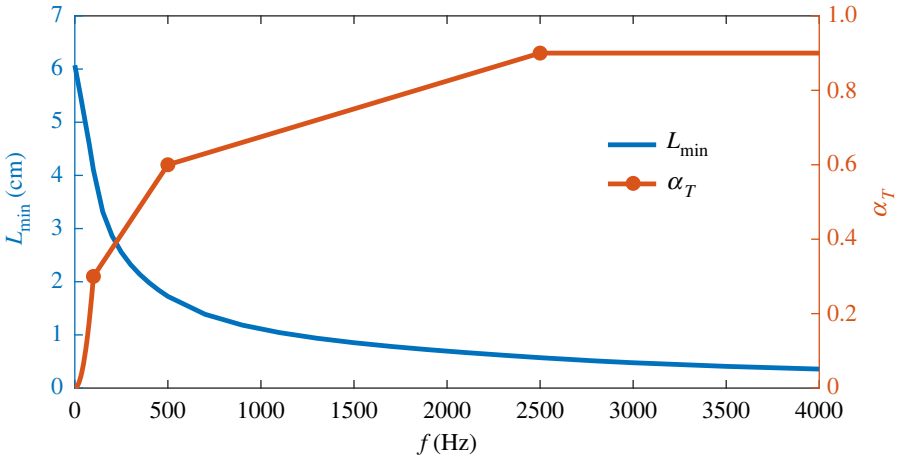

Figure 2. Target absorption spectrum α_T and the minimum length $L_{\min}$ evaluated from the contribution of α_T within the frequency range $[f, \infty)$. (Online version in colour.)

$\alpha_T = 30(f/10^3)^2$ when $f \leq 100$ Hz. For a higher frequency range, the target spectrum α_T is derived from interpolations

$$\alpha_T(f) = \begin{cases} 30\left(\frac{f}{10^3}\right)^2 & f \leq 100\,\text{Hz} \\ 0.75\left(\frac{f}{10^3}\right) + 0.225 & 100\,\text{Hz} \leq f \leq 500\,\text{Hz} \\ 0.15\left(\frac{f}{10^3}\right) + 0.525 & 500\,\text{Hz} \leq f \leq 2500\,\text{Hz} \\ 0.9 & f \geq 2500\,\text{Hz} \end{cases}. \tag{4.2}$$

With this target α_T, the minimum length is predicted from equation (4.1), which results in $L_{\min} = 6.1$ cm. The effect of the low-frequency spectrum of α_T on $L_{\min}$ is further studied through calculation of equation (4.1) within the frequency band $[f, \infty)$. The results are illustrated in figure 2. It is found that, although α_T is less than 0.3 below 100 Hz, the low-frequency spectrum still has a significant effect on $L_{\min}$. When we start the sum-rule integration at $f = 100$ Hz, $L_{\min}$ reduces to 4.1 cm, which is 30% lower than that predicted by the full spectrum. By contrast, the high-frequency spectrum (although α_T is close to one) has much less effect on $L_{\min}$. If we set $\alpha_T = 0$ for $f \geq 2500$ Hz, the predicted $L_{\min}$ is merely 10% less than 6.1 cm.

In the above calculations, the porosity $\phi = 1$ is used. For commonly used porous materials, ϕ is very close to unity as shown in [56]. For other in-series structures used within the waveguide, when ϕ is difficult to evaluate, $\phi = 1$ can be used as well to predict the lower bound of $L_{\min}$.

(b) Minimum volume of a ring-shaped muffler for a target transmission loss spectrum with grazing incident wave

We consider the transmission problem of a ring-shaped muffler with length L in the axial direction and thickness H in the radial direction, as illustrated in figure 3. This muffler is set in parallel of a circular waveguide whose radius is R_d. It is modelled as an equivalent material, with a rigid outer boundary at $r = R_d + H$. The muffler is assumed to be locally reacting so that there is only unidimensional radial wave within the equivalent material. Then the viscothermal losses within the material can be modelled by complex-valued effective parameters: the effective density and bulk modulus of the material are denoted by ρ_m and K_m, respectively. By contrast, losses in the main waveguide are neglected.

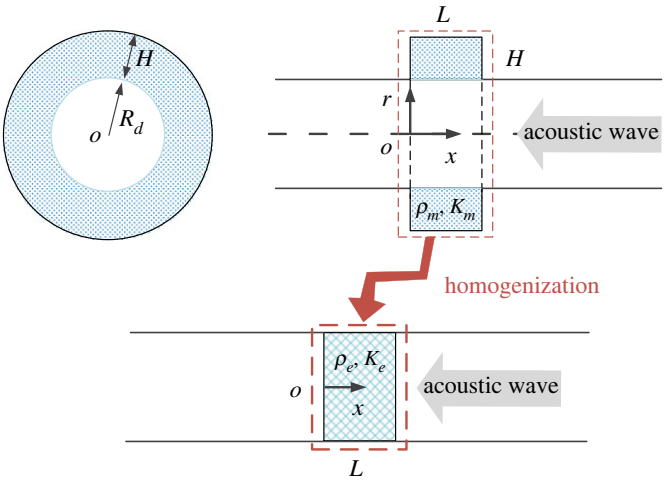

Figure 3. Effective layer introduced by a ring-shaped muffler in parallel of a circular waveguide. The muffler is filled with a uniform material whose effective density and bulk modulus are ρ_m and K_m, respectively. Via the homogenization method, the acoustic performance of the muffler can be well described by the layer with effective parameters ρ_e and K_e. (Online version in colour.)

Under these assumptions, the effect of the muffler on the wave propagation in the waveguide can be well described by introducing an effective layer with the same axial length L. Then the static and dynamic limits of the effective parameters of the layer could be evaluated and the sum rules in the unidimensional transmission problem can be directly applied. Via the zeroth-order homogenization scheme [39,40,54], the static limit of the effective density of the layer ($\rho_e(0)$) reduces to that of the medium within the waveguide, whereas the static limit of the effective bulk modulus ($K_e(0)$) can be expressed by that of each component weighted by the volume. It follows that

$$\frac{\rho_e(0)}{\rho_0} = 1 \tag{4.3a}$$

and

$$\frac{K_e(0)}{K_0} = 1 + \frac{V}{V_e}\frac{K_m(0)}{K_0} = 1 + \frac{V}{V_e}\frac{1}{\gamma\phi_m}, \tag{4.3b}$$

where $V_e = \pi R_d^2 L$ is the volume of the effective layer, $V = \pi(2R_d H + H^2)L$ is the volume of the ring-shaped material and ϕ_m is the porosity of the material. Another derivation of the acoustical response of the system via the transfer matrix method is provided in the electronic supplementary material. Because the imaginary part of the effective density is proportional to the steady flow resistivity in the static limit, equation (4.3*a*) implies that the effective layer is perfectly non-resistive ($\xi = 0$). Therefore, the sum rule (3.25*a*) can be directly used to evaluate the minimum length of the effective layer with the target transmission loss spectrum TL_T given. Note that under a grazing incident wave, c_∞ (or τ_∞) of the effective layer is usually difficult to evaluate. Here, $c_\infty = c_0$ (i.e. $\tau_\infty = 1$) is used as an approximation. With $\rho_e(0)$, $K_e(0)$ and c_∞ provided, the sum rule (3.25*a*) can be rewritten as

$$V_{\min} = \frac{c_0 R_d^2 \ln 10}{10\pi\gamma\phi_m}\int_{f_1}^{f_2}\frac{\mathrm{TL}_T(f)}{f^2}\,\mathrm{d}f, \tag{4.4}$$

where $V_{\min} = \min[\pi(2R_d H + H^2)L]$ denotes the minimum volume of the ring-shaped muffler.

We assume that the target transmission loss TL_T is larger than 2 dB, 12 dB, 8 dB and 2 dB at 250 Hz, 500 Hz, 1000 Hz and 2000 Hz, respectively. The radius of the circular waveguide R_d is assumed to be 5 cm. Similarly to the previous example, the TL_T spectrum under 250 Hz is

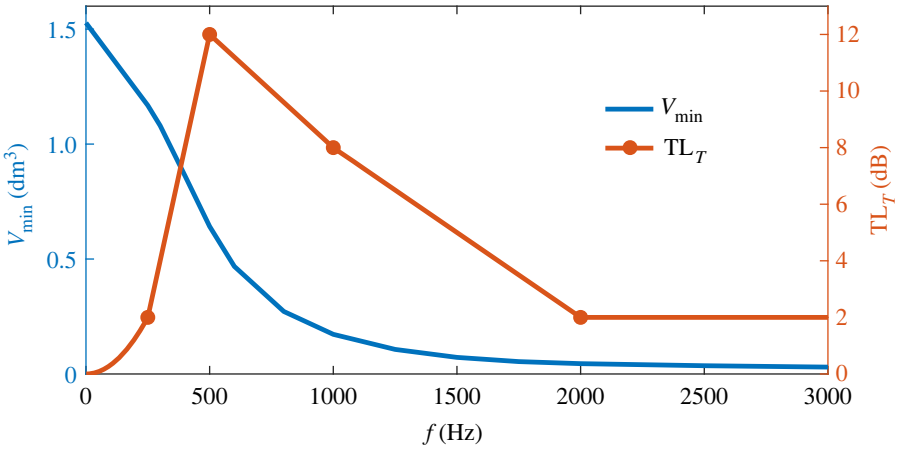

Figure 4. Target transmission loss spectrum TL_T and the minimum volume $V_{\min}$ evaluated from the contribution of TL_T within the frequency range $[f, \infty)$. (Online version in colour.)

important for the prediction of the minimum volume. Since $|T(\omega)|^2 = 1 - A\omega^2 + o(\omega^2)$ at low frequency, where A is a positive coefficient, the transmission loss also possesses the quadratic dependence on frequency near the static limit. Thus, the target spectrum TL_T is expressed by the following function:

$$\mathrm{TL}_T(f) = \begin{cases} 32\left(\frac{f}{10^3}\right)^2 & f \le 250\,\mathrm{Hz} \\ 40\left(\frac{f}{10^3}\right) - 8 & 250\,\mathrm{Hz} \le f \le 500\,\mathrm{Hz} \\ -8\left(\frac{f}{10^3}\right) + 16 & 500\,\mathrm{Hz} \le f \le 1000\,\mathrm{Hz} \\ -6\left(\frac{f}{10^3}\right) + 14 & 1000\,\mathrm{Hz} \le f \le 2000\,\mathrm{Hz} \\ 2 & f \ge 2000\,\mathrm{Hz} \end{cases}. \tag{4.5}$$

With TL_T provided, the effect of the given spectrum on the prediction of $V_{\min}$ can be analysed. Results of parametric studies are illustrated in figure 4, where $V_{\min}(f)$ is calculated by equation (4.4) within the frequency band $[f, \infty)$, and $\phi_m = 1$. If TL_T is approximated by zero when $f \le 250\,\mathrm{Hz}$, the underestimation of $V_{\min}$ is nearly 25%. In the opposite, the high-frequency spectrum of TL_T (e.g. $f > 1000\,\mathrm{Hz}$) does not contribute much to $V_{\min}$, as one would expect.

5. Conclusion

With the sum rules in lossy acoustical systems, the minimum size of a passive metamaterial is readily predicted from its target broadband response, which is of primary importance for guiding the design of subwavelength acoustical treatments.

In this work, the theory of Herglotz function is revisited and applied systematically to derive sum rules for unidimensional acoustical scattering problems, including the rigid/soft-boundary reflection and the transmission problems. The derivations in all the cases involve the following standard steps: (a) Identify non-negative valued functions (i.e. Herglotz functions) from the relevant response functions, considering either admittance/impedance passivity or scattering passivity of the system. (b) Analyse the asymptotic behaviours of these Herglotz functions in the static and dynamic limits. (c) Derive the sum rules from the coefficients of the asymptotic expansions.

In the rigid-boundary reflection problem, the recently derived constraint for the absorption coefficient in [18] is recovered. Moreover, a new constraint for the surface admittance is obtained.

In the soft-boundary reflection and the transmission problems, the asymptotic behaviours of Herglotz functions depend on the steady flow resistance of the effective material, i.e. $\xi = L\sigma/z_0$. Consequently, sum rules in these two problems exist merely when $\xi \to 0$ or $\xi \to \infty$, corresponding to cases in which the material is either non-resistive or highly resistive, respectively. Besides, in special cases where $\xi = 1$ or 2 in the soft-boundary reflection or the transmission problem, the absorption coefficients can reach their maximum static-limit values, 1 or 1/2, respectively, although the considered Herglotz functions do not admit sum rules.

Data accessibility. The data are provided in the electronic supplementary material [58].

Authors' contributions. Y.M.: conceptualization, investigation, methodology, validation, writing—original draft, writing—review and editing; V.R.-G.: conceptualization, investigation, methodology, validation, writing—review and editing; G.G.: conceptualization, investigation, methodology, validation, writing—review and editing; J.-P.G.: conceptualization, funding acquisition, investigation, methodology, project administration, validation, writing—review and editing; C.B.: validation, writing—review and editing; S.G.: validation, writing—review and editing; P.S.: conceptualization, validation, writing—review and editing.

All authors gave final approval for publication and agreed to be held accountable for the work performed therein.

Conflict of interest declaration. We declare we have no competing interests.

Funding. This work is supported by Valeo company and the ANR-RGC METARoom project (grant nos. ANR-18-CE08-0021 and RGC A-HKUST601/18).

Appendix A. Static/dynamic limits of the effective parameters

The losses of the system arise from viscothermal effects near the no-slip and isothermal boundaries. Here, we fix the discussion on an in-series material inside the waveguide. When side-branch structures are included, the asymptotic expansions of the effective parameters of the material preserve the same dependence on ω, but the coefficients should be interpreted differently.

For in-series material with porosity ϕ, the asymptotic expansions can be directly evaluated [41]. In the static limit $\omega \hat{\to} 0$,

$$\frac{\rho_e}{\rho_0} \hat{\to} \frac{1}{\phi}\left(\mathrm{i}\frac{C_1}{S_H^2} + C_2\right) + o(1) = \mathrm{i}\frac{\sigma}{\rho_0\omega} + \frac{C_2}{\phi} + o(1), \tag{A 1a}$$

$$\frac{c_e}{c_0} \hat{\to} (1-\mathrm{i})C_3 S_H + o(\sqrt{\omega}), \tag{A 1b}$$

$$\frac{z_e}{z_0} \hat{\to} \frac{(1+\mathrm{i})C_1C_3}{\phi S_H} + o\left(\frac{1}{\sqrt{\omega}}\right) \tag{A 1c}$$

and

$$\frac{K_e}{K_0} \hat{\to} \frac{2C_1C_3^2}{\phi} + o(1) = \frac{1}{\phi\gamma} + o(1), \tag{A 1d}$$

where C_1, C_2 and C_3 are positive real constants (see pp. 55–57 of [41]), $S_H = r_H\sqrt{\omega/\nu_0}$ is the shear number of the cross section [57], $\nu_0 = \mu_0/\rho_0$ is the kinematic viscosity of air. Note that, from equation (A 1*a*), the static limit of the density has a diverging imaginary part $\sim 1/\omega$. The real part tends to a constant and is written $C_2/\phi \equiv \mathrm{Re}[\rho_e(0)]/\rho_0$. According to equation (A 1*d*), the static limit of the bulk modulus is real-valued and is written $2C_1C_3^2/\phi = 1/(\phi\gamma) \equiv K_e(0)/K_0$.

Furthermore, in the dynamic limit $\omega \hat{\to} \infty$,

$$\frac{\rho_e}{\rho_0} \hat{\to} \frac{\tau_\infty}{\phi}\left[1 + (1+\mathrm{i})\frac{D_1}{S_H}\right] + o\left(\frac{1}{\sqrt{\omega}}\right), \tag{A 2a}$$

$$\frac{c_e}{c_0} \hat{\to} \frac{1}{\sqrt{\tau_\infty}}\left[1 - (1+\mathrm{i})\frac{D_2}{S_H}\right] + o\left(\frac{1}{\sqrt{\omega}}\right), \tag{A 2b}$$

$$\frac{z_e}{z_0} \hat{\to} \frac{\sqrt{\tau_\infty}}{\phi}\left[1 + \frac{(1+\mathrm{i})(D_1 - D_2)}{S_H}\right] + o\left(\frac{1}{\sqrt{\omega}}\right) \tag{A 2c}$$

and

$$\frac{K_e}{K_0} \hat{\to} \frac{1}{\phi}\left[1 + \frac{(1+\mathrm{i})(D_1 - 2D_2)}{S_H}\right] + o\left(\frac{1}{\sqrt{\omega}}\right), \tag{A 2d}$$

where D_1 and D_2 are positive real constants (see p. 71 of [41]), τ_∞ is the dynamic tortuosity. It is found that the dynamic limits of all these effective parameters are positive constants. Here, we denote $1/\sqrt{\tau_\infty} \equiv c_\infty/c_0$ and $\sqrt{\tau_\infty}/\phi \equiv z_\infty/z_0$.

Appendix B. Asymptotic performances of the Herglotz functions

(a) Rigid-boundary reflection problem

In the reflection problem with a rigid boundary, the relevant response functions are the surface admittance $\eta(\omega)$ and the reflection coefficient $R(\omega)$. Their asymptotic behaviours are given by

$$\eta(\omega) = \begin{cases} -\frac{\mathrm{i}\omega L}{c_0}\frac{K_0}{K_e(0)} + o(\omega), & \omega \hat{\to} 0 \\ \frac{z_0}{z_\infty} + o(1), & \omega \hat{\to} \infty \end{cases} \tag{B 1}$$

and

$$R(\omega) = \begin{cases} 1 + \frac{2\mathrm{i}\omega L}{c_0}\frac{K_0}{K_e(0)} + o(\omega), & \omega \hat{\to} 0 \\ \frac{z_\infty - z_0}{z_\infty + z_0} + o(1), & \omega \hat{\to} \infty \end{cases}. \tag{B 2}$$

The following two Herglotz functions are introduced: $H_1(\omega) = \mathrm{i}\eta(\omega)$ and $H_2(\omega) = -\mathrm{i}\log[R(\omega)B(\omega)]$. Their asymptotic expansions are written as

$$H_1(\omega) = \begin{cases} \frac{\omega L}{c_0}\frac{K_0}{K_e(0)} + o(\omega), & \omega \hat{\to} 0 \\ O(1), & \omega \hat{\to} \infty \end{cases} \tag{B 3}$$

and

$$H_2(\omega) = \begin{cases} \omega\left[\frac{2L}{c_0}\frac{K_0}{K_e(0)} + \sum_n \mathrm{Im}\left(\frac{1}{\omega_n}\right)\right] + o(\omega) \le \frac{2\omega L}{c_0}\frac{K_0}{K_e(0)} + o(\omega), & \omega \hat{\to} 0 \\ O(1), & \omega \hat{\to} \infty \end{cases}. \tag{B 4}$$

Note that the inequality in equation (B 4) is derived with $\mathrm{Im}(\omega_n) > 0$. From the above expansions, it is found that, for H_1:

$$a_1 = \frac{L}{c_0}\frac{K_0}{K_e(0)} \quad \text{and} \quad b_1 = 0. \tag{B 5}$$

And for H_2:

$$a_1 \le \frac{L}{c_0}\frac{K_0}{K_e(0)} \quad \text{and} \quad b_1 = 0. \tag{B 6}$$

(b) Soft-boundary reflection problem

In the soft-boundary reflection problem, the relevant response functions include the impedance $\zeta(\omega)$, the admittance $\eta(\omega)$ and the reflection coefficient $R(\omega)$. The asymptotic behaviours of these functions are as follows:

$$\zeta(\omega) = \begin{cases} \xi - \frac{\mathrm{i}\omega L}{c_0}\left\{\frac{\mathrm{Re}[\rho_e(0)]}{\rho_0} - \frac{\xi^2 K_0}{3K_e(0)}\right\} + o(\omega), & \omega \hat{\to} 0 \\ \frac{z_\infty}{z_0} + o(1), & \omega \hat{\to} \infty \end{cases}, \tag{B 7}$$

$$\eta(\omega) = \begin{cases} \frac{1}{\xi} - \frac{\mathrm{i}\omega L}{c_0}\left\{\frac{K_0}{3K_e(0)} - \frac{\mathrm{Re}[\rho_e(0)]}{\xi^2\rho_0}\right\} + o(\omega), & \omega \hat{\to} 0 \\ \frac{z_0}{z_\infty} + o(1), & \omega \hat{\to} \infty \end{cases} \tag{B 8}$$

and

$$R(\omega) = \begin{cases} \frac{\xi-1}{\xi+1} + \frac{2\mathrm{i}\omega L}{c_0}\frac{(\xi^2/3) - (K_e(0)/K_0)(\mathrm{Re}[\rho_e(0)]/\rho_0)}{(\xi+1)^2(K_e(0)/K_0)} + o(\omega), & \omega \hat{\to} 0 \\ \frac{z_\infty - z_0}{z_\infty + z_0} + o(1), & \omega \hat{\to} \infty \end{cases}, \tag{B 9}$$

in which $\xi = C_1 L\nu_0/(\phi c_0 r_H^2) = L\sigma/z_0$.

(i) Non-resistive material: $\xi \to 0$

When $\xi \to 0$, the Herglotz functions $H_1(\omega) = \mathrm{i}\zeta(\omega)$ and $H_2(\omega) = -\mathrm{i}\log[-R(\omega)B(\omega)]$ are considered. Their asymptotic expansions are

$$H_1(\omega) = \begin{cases} \frac{\omega L}{c_0}\frac{\mathrm{Re}[\rho_e(0)]}{\rho_0} + o(\omega), & \omega \hat{\to} 0 \\ O(1), & \omega \hat{\to} \infty \end{cases} \tag{B 10}$$

and

$$H_2(\omega) = \begin{cases} \omega\left\{\frac{2L}{c_0}\frac{\mathrm{Re}[\rho_e(0)]}{\rho_0} + \sum_n \mathrm{Im}\left(\frac{1}{\omega_n}\right)\right\} + o(\omega) \leq \frac{2\omega L}{c_0}\frac{\mathrm{Re}[\rho_e(0)]}{\rho_0} + o(\omega), & \omega \hat{\to} 0 \\ O(1), & \omega \hat{\to} \infty \end{cases}. \tag{B 11}$$

It follows that, for H_1:

$$a_1 = \frac{L}{c_0}\frac{\mathrm{Re}[\rho_e(0)]}{\rho_0} \quad \text{and} \quad b_1 = 0. \tag{B 12}$$

And for H_2:

$$a_1 \leq \frac{2L}{c_0}\frac{\mathrm{Re}[\rho_e(0)]}{\rho_0} \quad \text{and} \quad b_1 = 0. \tag{B 13}$$

(ii) Highly resistive material: $\xi \to \infty$

When $\xi \to \infty$, the Herglotz functions $H_1(\omega) = \mathrm{i}\eta(\omega)$, and $H_2(\omega) = -\mathrm{i}\log[R(\omega)B(\omega)]$ are used. It follows that

$$H_1(\omega) = \begin{cases} \frac{\omega L}{3c_0}\frac{K_0}{K_e(0)} + o(\omega), & \omega \hat{\to} 0 \\ O(1), & \omega \hat{\to} \infty \end{cases} \tag{B 14}$$

and

$$H_2(\omega) = \begin{cases} \omega\left[\frac{2L}{3c_0}\frac{K_0}{K_e(0)} + \sum_n \mathrm{Im}\left(\frac{1}{\omega_n}\right)\right] + o(\omega) \leq \frac{2\omega L}{3c_0}\frac{K_0}{K_e(0)} + o(\omega), & \omega \hat{\to} 0 \\ O(1), & \omega \hat{\to} \infty \end{cases}. \tag{B 15}$$

Therefore, for H_1:

$$a_1 = \frac{L}{3c_0}\frac{K_0}{K_e(0)} \quad \text{and} \quad b_1 = 0. \tag{B 16}$$

And for H_2:

$$a_1 \leq \frac{2L}{3c_0}\frac{K_0}{K_e(0)} \quad \text{and} \quad b_1 = 0. \tag{B 17}$$

(c) Transmission problem

In the transmission problem, $R^-(\omega) = R^+(\omega) \equiv R(\omega)$ and $T^-(\omega) = T^+(\omega) \equiv T(\omega)$ when we consider a symmetric single-layer material. The asymptotic behaviours of $R(\omega)$ and $T(\omega)$ are provided by

$$R(\omega) = \begin{cases} \frac{\xi}{\xi+2} + \frac{2\mathrm{i}\omega L}{c_0}\frac{(\xi^2/3)+\xi+1-(K_e(0)/K_0)(\mathrm{Re}[\rho_e(0)]/\rho_0)}{(\xi+2)^2(K_e(0)/K_0)} + o(\omega), & \omega \hat{\to} 0 \\ \frac{z_\infty - z_0}{z_\infty + z_0} + o(1), & \omega \hat{\to} \infty \end{cases} \tag{B 18}$$

and

$$T(\omega) = \begin{cases} \frac{2}{\xi+2} + \frac{2\mathrm{i}\omega L}{c_0}\frac{1+\xi[(\xi/6)-(K_e(0)/K_0)+1]+(K_e(0)/K_0)\{(\mathrm{Re}[\rho_e(0)]/\rho_0)-2\}}{(\xi+2)^2(K_e(0)/K_0)} + o(\omega), & \omega \hat{\to} 0 \\ o(1), & \omega \hat{\to} \infty \end{cases}. \tag{B 19}$$

(i) Non-resistive material: $\xi \to 0$

Consider a non-resistive material with $\xi \to 0$. The Herglotz functions $H_1(\omega) = \mathrm{i}[1 - T(\omega)]/[1 + T(\omega)]$ and $H_2(\omega) = -\mathrm{i}\log[T(\omega)B(\omega)]$ are used. Then the asymptotic expansions provide

$$H_1(\omega) = \begin{cases} \frac{\omega L}{4c_0}\left\{\frac{K_0}{K_e(0)} + \frac{\mathrm{Re}[\rho_e(0)]}{\rho_0} - 2\right\} + o(\omega), & \omega \hat{\to} 0 \\ O(1), & \omega \hat{\to} \infty \end{cases} \tag{B 20}$$

and

$$H_2(\omega) = \begin{cases} \omega\left\{\frac{L}{2c_0}\left\{\frac{K_0}{K_e(0)} + \frac{\mathrm{Re}[\rho_e(0)]}{\rho_0} - 2\right\} + \sum_n \mathrm{Im}\left(\frac{1}{\omega_n}\right)\right\} + o(\omega) \\ \le \omega\left\{\frac{L}{2c_0}\left\{\frac{K_0}{K_e(0)} + \frac{\mathrm{Re}[\rho_e(0)]}{\rho_0} - 2\right\}\right\} + o(\omega), & \omega \hat{\to} 0 \\ \frac{\omega L}{c_0}\left(\frac{c_\infty}{c_0} - 1\right) + o(\omega), & \omega \hat{\to} \infty \end{cases} . \tag{B 21}$$

It can be found that, for H_1:

$$a_1 = \frac{L}{4c_0}\left\{\frac{K_0}{K_e(0)} + \frac{\mathrm{Re}[\rho_e(0)]}{\rho_0} - 2\right\} \quad \text{and} \quad b_1 = 0. \tag{B 22}$$

And for H_2:

$$a_1 \le \frac{L}{2c_0}\left\{\frac{K_0}{K_e(0)} + \frac{\mathrm{Re}[\rho_e(0)]}{\rho_0} - 2\right\} \quad \text{and} \quad b_1 = \frac{L}{c_0}\left(\frac{c_\infty}{c_0} - 1\right). \tag{B 23}$$

(ii) Highly resistive material: $\xi \to \infty$

When the material is highly resistive ($\xi \to \infty$), Herglotz functions $H_1(\omega) = \mathrm{i}\eta(\omega) = \mathrm{i}[1 - R(\omega)]/[1 + R(\omega)]$ and $H_2(\omega) = -\mathrm{i}\log[R(\omega)B(\omega)]$ are used. Their asymptotic expansions are

$$H_1(\omega) = \begin{cases} \frac{\omega L}{3c_0}\frac{K_0}{K_e(0)} + o(\omega), & \omega \hat{\to} 0 \\ O(1), & \omega \hat{\to} \infty \end{cases} \tag{B 24}$$

and

$$H_2(\omega) = \begin{cases} \omega\left[\frac{2L}{3c_0}\frac{K_0}{K_e(0)} + \sum_n \mathrm{Im}\left(\frac{1}{\omega_n}\right)\right] + o(\omega) \le \frac{2\omega L}{3c_0}\frac{K_0}{K_e(0)} + o(\omega), & \omega \hat{\to} 0 \\ O(1), & \omega \hat{\to} \infty \end{cases} . \tag{B 25}$$

For H_1:

$$a_1 = \frac{L}{3c_0}\frac{K_0}{K_e(0)} \quad \text{and} \quad b_1 = 0. \tag{B 26}$$

And for H_2:

$$a_1 \le \frac{2L}{3c_0}\frac{K_0}{K_e(0)} + o(\omega) \quad \text{and} \quad b_1 = 0. \tag{B 27}$$

The asymptotic behaviours of H_1 and H_2 are exactly those in the soft-boundary reflection problem with $\xi \to \infty$.

References

1. Beltrami E. 1967 Linear dissipative systems, nonnegative definite distributional kernels, and the boundary values of bounded-real and positive-real matrices. *J. Math. Anal. Appl.* **19**, 231–246. (doi:10.1016/0022-247X(67)90118-7)
2. Bernland A, Luger A, Gustafsson M. 2011 Sum rules and constraints on passive systems. *J. Phys. A* **44**, 145205. (doi:10.1088/1751-8113/44/14/145205)
3. Srivastava A. 2021 Causality and passivity: from electromagnetism and network theory to metamaterials. *Mech. Mater.* **154**, 103710. (doi:10.1016/j.mechmat.2020.103710)
4. Khodavirdi H, Srivastava A. 2022 The analytical structure of acoustic and elastic material properties. *Wave Motion* **108**, 102837. (doi:10.1016/j.wavemoti.2021.102837)
5. Kronig RDL. 1926 On the theory of dispersion of X-rays. *J. Opt. Soc. Am.* **12**, 547–557. (doi:10.1364/JOSA.12.000547)

6. Kramers HA. 1927 La diffusion de la lumiere par les atomes. In *Atti Cong. Intern. Fisica* (*Proceedings of the International Congress of Physicists*), *11–20 September 1927, Como-Pavia-Rome*.
7. Bode HW. 1940 Relations between attenuation and phase in feedback amplifier design. *Bell Syst. Tech. J.* **19**, 421–454. (doi:10.1002/j.1538-7305.1940.tb00839.x)
8. Peiponen KE, Saarinen JJ. 2009 Generalized Kramers–Kronig relations in nonlinear optical-and THz-spectroscopy. *Rep. Prog. Phys.* **72**, 056401. (doi:10.1088/0034-4885/72/5/056401)
9. Bechhoefer J. 2011 Kramers–Kronig, Bode, and the meaning of zero. *Am. J. Phys.* **79**, 1053–1059. (doi:10.1119/1.3614039)
10. De Alfaro V, Fubini S, Rossetti G, Furlan G. 1966 Sum rules for strong interactions. *Phys. Lett.* **21**, 576–579. (doi:10.1016/0031-9163(66)91306-0)
11. Altarelli M, Dexter DL, Nussenzveig HM, Smith DY. 1972 Superconvergence and sum rules for the optical constants. *Phys. Rev. B* **6**, 4502–4509. (doi:10.1103/PhysRevB.6.4502)
12. Smith DY, Manogue CA. 1981 Superconvergence relations and sum rules for reflection spectroscopy. *J. Opt. Soc. Am.* **71**, 935–947. (doi:10.1364/JOSA.71.000935)
13. Bode HW. 1945 *Network analysis and feedback amplifier design*. New York, NY: Van Nostrand.
14. Fano RM. 1950 Theoretical limitations on the broadband matching of arbitrary impedances. *J. Franklin Inst.* **249**, 57–83. (doi:10.1016/0016-0032(50)90006-8)
15. King FW. 2009 *Hilbert transforms*, vol. **2**. Cambridge, UK: Cambridge University Press.
16. Rozanov KN. 2000 Ultimate thickness to bandwidth ratio of radar absorbers. *IEEE Trans. Antennas Propag.* **48**, 1230–1234. (doi:10.1109/8.884491)
17. Acher O, Bernard JML, Maréchal P, Bardaine A, Levassort F. 2009 Fundamental constraints on the performance of broadband ultrasonic matching structures and absorbers. *J. Acoust. Soc. Am.* **125**, 1995–2005. (doi:10.1121/1.3081529)
18. Yang M, Chen S, Fu C, Sheng P. 2017 Optimal sound-absorbing structures. *Mater. Horiz.* **4**, 673–680. (doi:10.1039/C7MH00129K)
19. Bravo T, Maury C. 2022 Causally-guided acoustic optimization of single-layer rigidly-backed micro-perforated partitions: theory. *J. Sound Vib.* **520**, 116634. (doi:10.1016/j.jsv.2021.116634)
20. Pascalutsa V. 2018 *Causality rules: a light treatise on dispersion relations and sum rules*. IOP Concise Physics. San Rafael, CA: Morgan & Claypool Publishers.
21. Seron MM, Braslavsky JH, Goodwin GC. 2012 *Fundamental limitations in filtering and control*. London, UK: Springer-Verlag London Ltd.
22. Nussenzveig HM. 1972 *Causality and dispersion relations*. New York, NY: Academic Press.
23. Bernland A. 2012 Integral identities for passive systems and spherical waves in scattering and antenna problems. PhD thesis, Department of Electrical and Information Technology, Lund University.
24. Gustafsson M. 2013 An overview of sum rules and physical limitations for passive metamaterial structures. In *META13, the 4th Int. Conf. on Metamaterials, Photonic Crystals and Plasmonics*, *Sharjah-Dubai, United Arab Emirates, 18–22 March*.
25. Cassier M, Milton GW. 2017 Bounds on Herglotz functions and fundamental limits of broadband passive quasistatic cloaking. *J. Math. Phys.* **58**, 071504. (doi:10.1063/1.4989990)
26. Nedic M, Ehrenborg C, Ivanenko Y, Ludvig-Osipov A, Nordebo S, Luger A, Jonsson L, Sjöberg D, Gustafsson M. 2020 *Herglotz functions and applications in electromagnetics*, Electromagnetics and Radar, pp. 491–514. Institution of Engineering and Technology.
27. Yang M, Sheng P. 2017 Sound absorption structures: from porous media to acoustic metamaterials. *Ann. Rev. Mater. Res.* **47**, 83–114. (doi:10.1146/annurev-matsci-070616-124032)
28. Jiménez N, Romero-García V, Pagneux V, Groby JP. 2017 Rainbow-trapping absorbers: broadband, perfect and asymmetric sound absorption by subwavelength panels for transmission problems. *Sci. Rep.* **7**, 1–12. (doi:10.1038/s41598-017-13706-4)
29. Romero-García V, Jiménez N, Theocharis G, Achilleos V, Merkel A, Richoux O, Tournat V, Groby JP, Pagneux V. 2020 Design of acoustic metamaterials made of Helmholtz resonators for perfect absorption by using the complex frequency plane. *C. R. Phys.* **21**, 713–749. (doi:10.5802/crphys.32)
30. Huang S, Zhou Z, Li D, Liu T, Wang X, Zhu J, Li Y. 2020 Compact broadband acoustic sink with coherently coupled weak resonances. *Sci. Bull.* **65**, 373–379. (doi:10.1016/j.scib.2019.11.008)

31. Boulvert J, Humbert T, Romero-García V, Gabard G, Fotsing ER, Ross A, Mardjono J, Groby JP. 2022 Perfect, broadband, and sub-wavelength absorption with asymmetric absorbers: realization for duct acoustics with 3D printed porous resonators. *J. Sound Vib.* **523**, 116687. (doi:10.1016/j.jsv.2021.116687)
32. Seo SH, Kim YH, Kim KJ. 2018 Design of silencer using resonator arrays with high sound pressure and grazing flow. *Appl. Acoust.* **138**, 188–198. (doi:10.1016/j.apacoust.2018.04.001)
33. Ghaffarivardavagh R, Nikolajczyk J, Anderson S, Zhang X. 2019 Ultra-open acoustic metamaterial silencer based on Fano-like interference. *Phys. Rev. B* **99**, 024302. (doi:10.1103/PhysRevB.99.024302)
34. Jiménez N, Cox TJ, Romero-García V, Groby JP. 2017 Metadiffusers: deep-subwavelength sound diffusers. *Sci. Rep.* **7**, 1–12. (doi:10.1038/s41598-017-05710-5)
35. Ballestero E, Jimenez N, Groby JP, Aygun H, Dance S, Romero-García V. 2021 Metadiffusers for quasi-perfect and broadband sound diffusion. *Appl. Phys. Lett.* **119**, 044101. (doi:10.1063/5.0053413)
36. Craster RV, Guenneau S. 2012 *Acoustic metamaterials: negative refraction, imaging, lensing and cloaking*. Dordrecht, the Netherlands: Springer.
37. Deymier PA. 2013 *Acoustic metamaterials and phononic crystals*. Berlin, Heidelberg, Germany: Springer.
38. Gan WS. 2017 *New acoustics based on metamaterials*. Berlin, Germany: Springer.
39. Romero-Garcia V, Hladky-Hennion AC (eds). 2019 *Fundamentals and applications of acoustic metamaterials: from seismic to radio frequency*. Hoboken, NJ: John Wiley & Sons, Inc.
40. Jiménez N, Umnova O, Groby JP, editors. 2021 *Acoustic waves in periodic structures, metamaterials, and porous media: from fundamentals to industrial applications*. Cham: Springer.
41. Allard J, Atalla N. 2009 *Propagation of sound in porous media: modelling sound absorbing materials*, 2nd edn. Chichester, UK: John Wiley & Sons Ltd.
42. Kinsler LE, Frey AR, Coppens AB, Sanders JV. 2000 *Fundamentals of acoustics*. Hoboken, NJ: John Wiley & Sons Inc.
43. Blauert J, Laws P. 1978 Group delay distortions in electroacoustical systems. *J. Acoust. Soc. Am.* **63**, 1478–1483. (doi:10.1121/1.381841)
44. Merkel A, Theocharis G, Richoux O, Romero-García V, Pagneux V. 2015 Control of acoustic absorption in one-dimensional scattering by resonant scatterers. *Appl. Phys. Lett.* **107**, 244102. (doi:10.1063/1.4938121)
45. Jiménez N, Romero-García V, Pagneux V, Groby JP. 2017 Quasiperfect absorption by subwavelength acoustic panels in transmission using accumulation of resonances due to slow sound. *Phys. Rev. B* **95**, 014205. (doi:10.1103/PhysRevB.95.014205)
46. Romero-García V, Jiménez N, Groby JP, Merkel A, Tournat V, Theocharis G, Richoux O, Pagneux V. 2020 Perfect absorption in mirror-symmetric acoustic metascreens. *Phys. Rev. Appl.* **14**, 054055. (doi:10.48550/arXiv.2007.08393)
47. Mak HY, Zhang X, Dong Z, Miura S, Iwata T, Sheng P. 2021 Going beyond the causal limit in acoustic absorption. *Phys. Rev. Appl.* **16**, 044062. (doi:10.1103/PhysRevApplied.16.044062)
48. Carrier GF, Krook M, Pearson CE. 2005 *Functions of a complex variable: theory and technique*. Philadelphia, PA: SIAM.
49. Yang M, Meng C, Fu C, Li Y, Yang Z, Sheng P. 2015 Subwavelength total acoustic absorption with degenerate resonators. *Appl. Phys. Lett.* **107**, 104104. (doi:10.1063/1.4930944)
50. Lafarge D. 1993 Propagation du son dans les matériaux poreux à structure rigide saturés par un fluide viscothermique: définition de paramètres géométriques, analogie électromagnétique, temps de relaxation. PhD thesis, Université du Maine, Le Mans, France.
51. Lafarge D. 2006 *Matériaux et acoustique, I propagation des ondes acoustiques*. Paris: Lavoisier.
52. Willis J. 1981 Variational principles for dynamic problems for inhomogeneous elastic media. *Wave Motion* **3**, 1–11. (doi:10.1016/0165-2125(81)90008-1)
53. Merkel A, Romero-García V, Groby JP, Li J, Christensen J. 2018 Unidirectional zero sonic reflection in passive $\mathcal{PT}$-symmetric Willis media. *Phys. Rev. B* **98**, 201102. (doi:10.1103/PhysRevB.98.201102)
54. Groby JP, Malléjac M, Merkel A, Romero-García V, Tournat V, Torrent D, Li J. 2021 Analytical modeling of one-dimensional resonant asymmetric and reciprocal acoustic structures as Willis materials. *New J. Phys.* **23**, 053020. (doi:10.1088/1367-2630/abfab0)
55. Ablowitz MJ, Fokas AS, Fokas AS. 2003 *Complex variables: introduction and applications*. Cambridge, UK: Cambridge University Press.

56. Niskanen M, Groby JP, Duclos A, Dazel O, Le Roux JC, Poulain N, Huttunen T, Lähivaara T. 2017 Deterministic and statistical characterization of rigid frame porous materials from impedance tube measurements. *J. Acoust. Soc. Am.* **142**, 2407–2418. (doi:10.1121/1.5008742)
57. Peters MCAM, Hirschberg A, Reijnen AJ, Wijnands APJ. 1993 Damping and reflection coefficient measurements for an open pipe at low Mach and low Helmholtz numbers. *J. Fluid Mech.* **256**, 499–534. (doi:10.1017/S0022112093002861)
58. Meng Y, Romero-García V, Gabard G, Groby J-P, Bricault C, Goudé S, Sheng P. 2022 Fundamental constraints on broadband passive acoustic treatments in unidimensional scattering problems. Figshare. (doi:10.6084/m9.figshare.c.6176259)

Supplementary material for Fundamental constraints on broadband passive acoustic treatments in unidimensional scattering problems

Yang Meng, Vicente Romero-García, Gwénaël Gabard, Jean-Philippe Groby, Charlie Bricault, Sébastien Goudé, and Ping Sheng

1 Validations and parametric studies of the sum rules

In this section, two types of air-saturated porous materials are employed to study and validate all the derived sum rules for a single-layer material. Specifically, soft polyurethane foam (SPF) and glass wool are considered, which have low and high steady flow resistivity respectively and can be used to construct a non-resistive and a highly resistive layer. The structural parameters of these materials are listed in table 1, which are from the experimental studies in [1].

Table 1: Structural parameters of soft polyurethane foam (SPF) and glass wool.

	ϕ	τ_∞	Λ (μm)	Λ' (μm)	q_0 (10^{-9}m^2)	q_0' (10^{-9}m^2)
SPF	1.00	1.04	273	550	8.94	14.30
glass wool	0.96	1.00	37	100	0.39	0.58

We follow the same steps in all the validations: (a) choose a specific material with a given length so that $\xi = L\sigma/z_0$ is either close to zero or much larger than unity; (b) calculate the considered response function; (c) predict the total length from the sum rule; (d) compare the predicted length and the given length.

In particular, sum rules of the first type (derived from admittance/impedance passivity) are equations rather than inequalities. Thus, the predicted lengths should be exactly the given lengths in these cases. Otherwise, the predicted lengths should be less than the given lengths when the lengths are predicted from sum rules of the second type or from either type but with finite frequency interval (in the following computations we consider both the full frequency range from 0 Hz to infinity and the audible range from 20 Hz to 20 kHz).

1.1 Causal models of effective parameters of air-saturated porous media

To predict the effective parameters of an air-saturated porous medium, we use the models from [2, 3, 4]

$$\frac{\rho_\mathrm{e}(\omega)}{\rho_0} = \frac{\tau_\infty}{\phi} - \frac{\nu_0}{\mathrm{i}\omega q_0}\sqrt{1 - \frac{\mathrm{i}\omega}{\nu_0}\left(\frac{2\tau_\infty q_0}{\phi\Lambda}\right)^2}, \tag{1a}$$

$$\frac{K_\mathrm{e}(\omega)}{K_0} = \frac{1/\phi}{\gamma - \dfrac{\gamma - 1}{1 - \dfrac{\nu_0\phi}{\mathrm{i}\omega q_0'\mathrm{Pr}}\sqrt{1 - \dfrac{\mathrm{i}\omega\mathrm{Pr}}{\nu_0}\left(\dfrac{2q_0'}{\phi\Lambda'}\right)^2}}}, \tag{1b}$$

where $q_0 = \mu_0/\sigma$ is the static viscous permeability, q_0' is the static thermal permeability, Pr is the Prandtl number, Λ and Λ' are the characteristic viscous and thermal lengths respectively. In contrast to empirical

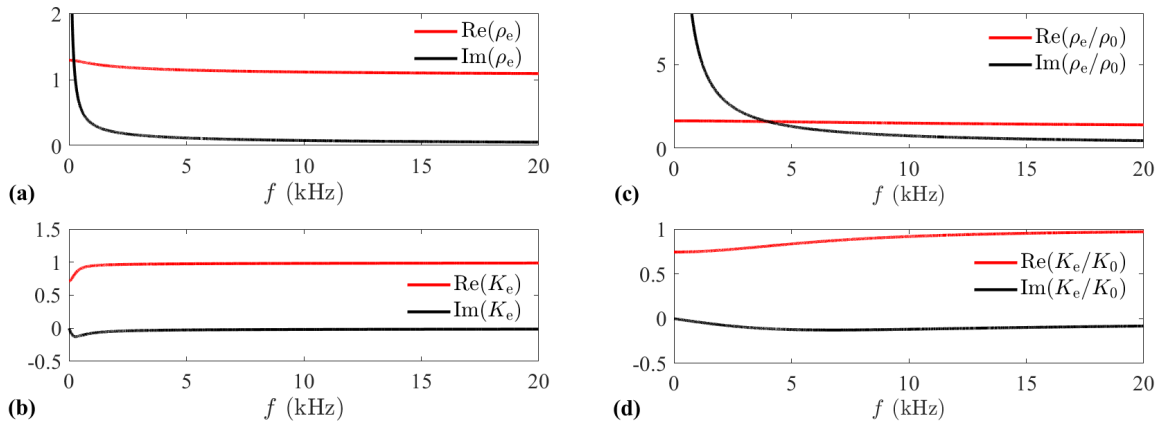

Figure 1: Effective parameters of the two materials. SPF: (a) effective density; (b) effective bulk modulus. Glass wool: (c) effective density; (d) effective bulk modulus.

formulas which mainly work in the moderate frequency range (e.g. [5]), the above models predict the right asymptotic behaviors in the static/dynamic limits, and moreover, satisfy causality (see also [6] and chapter 5 of [7]. Therefore, equations (1) are used to validate the sum rules derived in this work. The effective parameters of SPF and wool are then calculated by equations (1). Results are shown in figure 1.

1.2 Validations of sum rules for a non-resistive material

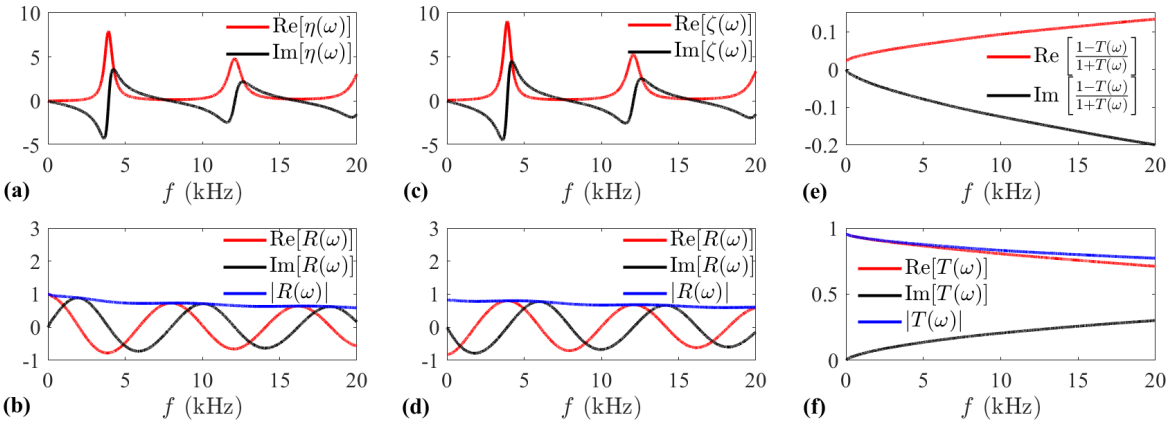

Figure 2: Acoustical response of the SPF layer. In the rigid-boundary reflection problem: (a) specific acoustic admittance; (b) reflection coefficient. In the soft-boundary reflection problem: (c) specific acoustic impedance; (d) reflection coefficient. In the transmission problem: (e) response function built from the transmission coefficient; (f) transmission coefficient.

To validate the sum rules for a non-resistive material, we consider a 2 cm layer of SPF. In this case, $\xi = 0.096 \ll 1$. The relevant response functions in reflection and transmission problems are derived and shown in figure 2. For the rigid-boundary reflection problem, the sum rules given by equations (3.4) in the main text can be readily validated. However, in the soft-boundary reflection problem, sum rules (3.11) hold merely in the limit $\xi \to 0$. Considering ξ as a finite small quantity, the following modified

Table 2: The total/minimum lengths of the SPF layer (whose length is 2 cm) predicted by sum rules.

	Sum rules	$L_{\min}$ (20 $\sim$ 20k Hz)	L or $L_{\min}$ (0 $\sim \infty$ Hz)
Rigid-boundary reflection problem	H_1: equation (3.4a)	1.8 cm	2.0 cm
	H_2: equation (3.4b)	0.6 cm	0.7 cm
Soft-boundary reflection problem	H_1: equation (3.11a)	1.9 cm	2.0 cm
	H_2: equation (3.11b)	0.2 cm	0.2 cm
Transmission problem	H_1: equation (3.21a)	1.6 cm	2.0 cm
	H_2: equation (3.21b)	1.7 cm	2.0 cm

forms of Herglotz functions are used in the computations to ensure the convergence of the integration:

$$H_1(\omega) = \mathrm{i}\left[\zeta(\omega) - \zeta(0)\right], \tag{2a}$$

$$H_2(\omega) = -\mathrm{i}\log\left[\frac{R(\omega)B(\omega)}{R(0)}\right], \tag{2b}$$

where the static limits are expressed as $\zeta(0) = \xi$ and $R(0) = (\xi-1)/(\xi+1)$. Similarly, in the transmission problem, the Herglotz functions used in the sum rules (3.21) are rewritten as

$$H_1(\omega) = \mathrm{i}\left[\frac{1-T(\omega)}{1+T(\omega)} - \frac{1-T(0)}{1+T(0)}\right], \tag{3a}$$

$$H_2(\omega) = -\mathrm{i}\log\left[\frac{T(\omega)B(\omega)}{T(0)}\right], \tag{3b}$$

where $T(0) = 2/(2+\xi)$. The prediction results on the total length or minimum length of the layer using different sum rules are collected in table 2.

1.3 Validations of sum rules for a highly resistive material

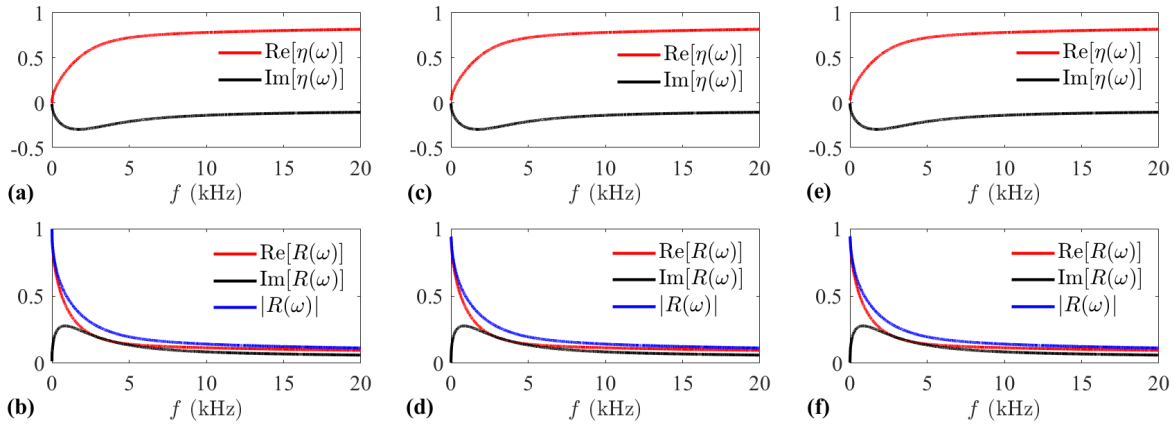

Figure 3: Acoustical response of the glass wool layer. In the rigid-boundary reflection problem: (a) specific acoustic admittance; (b) reflection coefficient. In the soft-boundary reflection problem: (c) specific acoustic admittance; (d) reflection coefficient. In the transmission problem: (e) specific acoustic admittance; (f) reflection coefficient.

To validate the sum rules for a highly resistive material, a thick layer of glass wool (0.3 m) is considered. In this case, $\xi = 33.21 \gg 1$. The considered response functions in all the cases are shown in figure 3. The sum rules given by equations (3.4) in the rigid-boundary reflection problem can be readily validated. Whereas in the soft-boundary reflection problem and the transmission problem, modified forms of Herglotz functions should be employed in the sum rules (in both case the sum rules are given by equations (3.16)):

$$H_1(\omega) = \mathrm{i}\left[\eta(\omega) - \eta(0)\right], \tag{4a}$$

$$H_2(\omega) = -\mathrm{i}\log\left[\frac{R(\omega)B(\omega)}{R(0)}\right], \tag{4b}$$

where $\eta(0) = 1/\xi$, $R(0) = (\xi-1)/(\xi+1)$ for the soft-boundary reflection problem, and $\eta(0) = 1/(1+\xi)$, $R(0) = \xi/(\xi+2)$ for the transmission problem. Validation results are provided in table 3.

Table 3: The total/minimum lengths of the glass wool layer (length 0.3 m) predicted by sum rules.

	Sum rules	$L_{\min}$ ($20 \sim 20$k Hz)	L or $L_{\min}$ ($0 \sim \infty$ Hz)
Rigid-boundary reflection problem	H_1: equation (3.4a)	0.12 m	0.30 m
	H_2: equation (3.4b)	0.12 m	0.30 m
Soft-boundary reflection problem	H_1: equation (3.16a)	0.24 m	0.30 m
	H_2: equation (3.16b)	0.24 m	0.30 m
Transmission problem	H_1: equation (3.16a)	0.24 m	0.30 m
	H_2: equation (3.16b)	0.24 m	0.30 m

2 Transfer matrix modelling of the ring-shaped muffler

When the total length (L) of a ring-shaped muffler is much less than the considered wavelength, the effect of the material can be modelled by a point surface impedance ζ_{m}, which is located at $x = L/2$. Suppose that the muffler is locally reacting so that only 1D radial waves exist inside the material. Then, the surface impedance is expressed by

$$\zeta_{\mathrm{m}} \equiv \left(\frac{p}{z_0 u}\right)_{r=R_{\mathrm{d}}} = \mathrm{i}\frac{z_{\mathrm{m}}}{z_0}\frac{J_1(k_{\mathrm{m}}r_2)N_0(k_{\mathrm{m}}r_1) - J_0(k_{\mathrm{m}}r_1)N_1(k_{\mathrm{m}}r_2)}{J_1(k_{\mathrm{m}}r_1)N_1(k_{\mathrm{m}}r_2) - J_1(k_{\mathrm{m}}r_2)N_1(k_{\mathrm{m}}r_1)}, \tag{5}$$

where $r_1 = R_{\mathrm{d}}$ and $r_2 = H + R_{\mathrm{d}}$ are the inner and outer radii, $z_{\mathrm{m}} = \rho_{\mathrm{m}}c_{\mathrm{m}}$ and $k_{\mathrm{m}} = \omega/c_{\mathrm{m}}$ are the effective impedance and wavenumber of the material, $J_{0,1}$ and $N_{0,1}$ are Bessel functions of first and second kinds, respectively. The transfer matrix of the system is

$$\begin{bmatrix} P(L) \\ U(L) \end{bmatrix} = \mathbf{T}_1\mathbf{T}_2\mathbf{T}_3 \begin{bmatrix} P(0) \\ U(0) \end{bmatrix} \equiv \mathbf{T} \begin{bmatrix} P(0) \\ U(0) \end{bmatrix}, \tag{6}$$

in which

$$\mathbf{T}_1 = \mathbf{T}_3 = \begin{bmatrix} \cos(k_0L/2) & \mathrm{i}\sin(k_0L/2) \\ \mathrm{i}\sin(k_0L/2) & \cos(k_0L/2) \end{bmatrix}, \quad \text{and} \quad \mathbf{T}_2 = \begin{bmatrix} 1 & 0 \\ -\dfrac{2L}{R_{\mathrm{d}}}\dfrac{1}{\zeta_{\mathrm{m}}} & 1 \end{bmatrix}. \tag{7}$$

Note that the viscothermal losses inside the waveguide have been neglected in $\mathbf{T}_1$ and $\mathbf{T}_3$.

References

[1] M. Niskanen, J.-P. Groby, A. Duclos, O. Dazel, J. C. Le Roux, N. Poulain, T. Huttunen, and T. Lähivaara. Deterministic and statistical characterization of rigid frame porous materials from

impedance tube measurements. *The Journal of the Acoustical Society of America*, 142(4):2407–2418, 2017.

[2] David Linton Johnson, Joel Koplik, and Roger Dashen. Theory of dynamic permeability and tortuosity in fluid-saturated porous media. *Journal of Fluid Mechanics*, 176:379–402, 1987.

[3] Yvan Champoux and Jean-F. Allard. Dynamic tortuosity and bulk modulus in air-saturated porous media. *Journal of Applied Physics*, 70(4):1975–1979, 1991.

[4] Denis Lafarge, Pavel Lemarinier, Jean F. Allard, and Viggo Tarnow. Dynamic compressibility of air in porous structures at audible frequencies. *The Journal of the Acoustical Society of America*, 102(4):1995–2006, 1997.

[5] M. E. Delany and E. N. Bazley. Acoustical properties of fibrous absorbent materials. *Applied acoustics*, 3(2):105–116, 1970.

[6] Z.E.A. Fellah, S. Berger, W. Lauriks, and C. Depollier. Verification of Kramers–Kronig relationship in porous materials having a rigid frame. *Journal of Sound and Vibration*, 270(4):865–885, 2004.

[7] J Allard and N Atalla. *Propagation of sound in porous media: modelling sound absorbing materials.* John Wiley & Sons, 2nd edition, 2009.